
WIND

2010 Senior Review Proposal

Adam Szabo
NASA GSFC
Project Scientist/Presenter

Michael R. Collier
NASA GSFC
Deputy Project Scientist

EXECUTIVE SUMMARY

NASA launched the *Wind* spacecraft in November, 1994 to the Earth's L1 Lagrange point as the interplanetary component of the Global Geospace Science Program within the International Solar Terrestrial Physics (ISTP) program. The spin stabilized spacecraft, with its spin axis pointing ecliptic north, carries eight instrument suites that provide comprehensive measurement of particles from solar wind thermal populations to the solar energetic component, and of fields from DC magnetic to radio waves and γ -rays. All of the instrument suites continue to provide valuable scientific observations completely available to the public, with the exception of one of the γ -ray instruments (TGRS).

The *Wind* instrument suite provides comprehensive and also uniquely high time resolution in-situ solar wind measurements that enable the investigation of wave-particle interactions. Thus *Wind* science investigations will continue to constrain the theories of solar wind and energetic particle acceleration processes and focus the science objectives of the upcoming *Solar Probe+* and *Solar Orbiter* missions. Once these new missions are launched, the high quality *Wind* in-situ observations will enable the connection of the 1 AU solar wind to its coronal source (see Figure 1.).

Moreover, *Wind* is the only near-Earth spacecraft equipped with radio waves instrumentation. Thus, together with its robust, multiply redundant solar wind observations, *Wind* is an ideal 3rd vantage point for



Figure 1. *Wind* will provide the 1 AU baseline for the upcoming *Solar Probe+* and *Solar Orbiter* missions and serve as a 3rd point solar wind observatory enhancing the science return of the STEREO mission. [J. Rumburg]

the STEREO mission. As the two STEREO spacecraft continue to increase their longitudinal separation from Earth reaching diametrically opposing positions from the Sun, *Wind* – located half way between them – will still continue to enable stereoscopic solar wind structure and radio triangulation studies (see Figure 1). *Wind*, together with SOHO, will also serve as a backup to one of the STEREO spacecraft.

Wind data have been critical to a wide range of studies from solar-heliosphere and heliosphere-magnetosphere connection to fundamental space research resulting in over 150 publications since the last Senior Review (only 2 years ago), listed on the *Wind* project Web page (wind.nasa.gov). The new results span all three heliophysics research objectives as described in the *Science Plan for NASA's Science Mission Directorate 2007-2016* and include the discovery of 1 AU signatures of a solar wind acceleration process, the understanding of energetic electron acceleration and the mapping of the complex internal structure of interplanetary coronal mass ejections (ICMEs).

Though some of the new results stem from *Wind* observations alone, most capitalize on multi-spacecraft measurements that treat all the heliophysics assets as a single great observatory. In fact, *Wind* team members have been leading the development of the new, distributed heliophysics data environment, including the Virtual Heliophysics Observatory (VHO) that connects the elements of the Heliophysics Great Observatory into a single system.

Even though *Wind* is now more than 15 years old, the mission promises a host of new discoveries. The time period covered by this proposal includes the rise to the next solar maximum. Because of its longevity, *Wind* observations will allow researchers to compare solar wind activity between solar cycles 22, 23 and 24 without needing to compensate for changing instrumentation and calibration. With its ample fuel reserves, sufficient for nearly 60 years, *Wind* will also continue to provide accurate solar wind input for magnetospheric studies (supporting MMS and RBSP) and serve as the 1 AU reference point for both inner heliospheric (MESSENGER, *Solar Orbiter*, and *Solar Probe+*) and outer heliospheric (*Voyager*, IBEX) investigations. Finally, *Wind* will continue to critically support other NASA missions, such as STEREO, RHESSI, ACE, LRO, SWIFT and *Fermi*.

The *Wind* science data products are publicly served directly from the instrument team sites. To aid the science user community, a single project web page has been developed with links to and descriptions of the large number of *Wind* data products (<http://wind.nasa.gov>). *Wind* is also an active participant in the development of the VHO that will make data queries even more user friendly.

Finally, *Wind* also has a real-time space weather warning mode that currently is used only during the daily 2-3 hour long science telemetry downlink to DSN. The *Wind* mission operation team is evaluating the option of keeping this real-time data stream on continuously. While the *Wind* real-time telemetry does require large (~30m) ground antennas, it is an invaluable backup to the ACE space weather beacon.

Rationale for Continuing the Wind Mission

- *Wind* continues to provide unique and robust solar wind measurements
- *Wind* provides high time resolution measurements that can serve as the 1 AU reference for *Solar Probe+* and *Solar Orbiter*.
- *Wind* is a 3rd solar wind vantage point for STEREO providing a backup capability and the continued possibility of stereoscopic observations.
- *Wind* and ACE together provide a reasonable probability of maintaining 24/7 near-Earth solar wind monitoring capabilities for NASA into the next decade.
- *Wind* and ACE are complementary not identical. Thus both are needed to provide complete near-Earth, 1 AU baseline observations for current and future NASA deep space missions.
- *Wind* still has redundant systems and instruments and enough fuel for 60 years.
- *Wind's* scientific productivity remains high and its observations continue to lead to significant scientific discoveries for all three research objectives of NASA's SMD.

TABLE OF CONTENTS

Executive Summary	1
Table of Contents	3
1. Introduction	4
1.1 Historical Background	4
1.2 Current Status	4
1.3 Unique Capabilities of <i>Wind</i>	4
1.4 Heliophysics Great Observatory	6
1.5 Living With a Star Program	6
2. Science Accomplishments and Goals	6
2.1 Heliophysics Objective #1: Fundamental Physical Processes	7
2.1.1 Understanding the origin and acceleration of the solar wind	7
2.1.2 Understanding reconnection in the solar wind	9
2.1.3 Understanding the acceleration and transport of solar energetic particles	10
2.2 Heliophysics Objective #2: The Evolution of Solar Transients in the Heliosphere	14
2.2.1 The long and quiet solar minimum	14
2.2.2 Interplanetary Coronal Mass ejections (ICMEs) and their driven shocks	15
2.3 Heliophysics Objective #3: Geomagnetic Impact	19
2.3.1 Solar wind disturbances impacting the Earth's magnetosphere	19
2.3.2 Forecasting the geomagnetic impact of magnetic clouds	20
3. <i>Wind</i> Support for Other missions	20
3.1 Wind and STEREO	21
3.2 Wind and ACE	21
3.3 Wind and RHESSI	21
3.4 Wind and IBEX, Voyagers, MESSENGER	22
3.5 Wind and ARTHEMIS, Cluster	22
3.6 Wind and RBSP, MMS	22
3.7 Wind and Swift, Fermi	22
4. Technical and Budget Section	23
4.1 Spacecraft Health	23
4.2 Instrument Status	23
4.3 Ground Operations	23
4.4 In-Guide Budget	24
4.4.1 Mission Operations	25
4.4.2 Science Data Production	25
References	26
Appendix A: STEREO/IMPACT - Wind Education and Public Outreach Program	29
Appendix B: Wind Legacy Mission Archive Plan	33
Acronyms	38

1. INRTODUCTION

1.1 Historical Background

The *Wind* spacecraft was launched in November, 1994 as the interplanetary component of the Global Geospace Science (GGS) Program within ISTP. *Wind's* original purpose was (1) to make accurate in situ measurements of interplanetary conditions upstream of the magnetosphere to complement measurements made in the magnetosphere by *Polar* and *Geotail* and (2) to remotely sense interplanetary disturbances for possible future predictive purposes. The instruments were therefore designed to make highly accurate solar wind measurements.

After a number of years at the L1 Lagrange point, *Wind* performed a series of orbital maneuvers to take it to various scientifically valuable observational points. In 1999, *Wind* executed a number of magnetospheric petal orbits that took it to the rarely sampled geomagnetic high latitudes. Between 2000 and 2002, *Wind* moved further and further away from the Sun-earth line (and ACE) reaching 350 R_E to the side in a distant prograde orbit. Finally, in 2003, it completed an L2 campaign taking the spacecraft more than 250 R_E downstream of Earth and $\sim 500 R_E$ downstream of ACE to investigate solar wind evolution and magnetotail phenomena. Since 2004, *Wind* has remained at L1 where it will stay for the foreseeable future.

1.2 Current Status

The *Wind* spacecraft continues to operate in good health. In 2000, the team successfully reconfigured the communications system to enhance the telemetry margin. Reliance on a single digital tape recorder since 1997 has never hampered operations, and the team took measures to minimize its use in order to extend tape recorder life as long as possible.

Seven of the eight *Wind* instruments, including all of the particles and fields instruments, remain largely or fully operational. Specifically, the EPACT, high energy particle and SMS solar wind composition instruments suffered some degradation, but both continue to provide valuable measurements. The SWE electron instrument required some reconfiguration to maintain its capabilities and the TGRS γ -ray detector, well beyond its design life, has been turned off. For technical details see Section 4.2. All the other instruments operate nominally. Thus, the net loss in capability remains minimal and the *Wind*

instruments continue to provide definitive and continuous measurements of the solar wind.

The joint *Wind-Polar-Geotail* mission operation center resides at Goddard. However, with the retirement of the *Polar* spacecraft, maintaining this legacy system is no longer cost effective. Design and development work is almost complete for a new, combined *Wind*, ACE and TRACE multi-mission operations center (MMOC), also at Goddard, with an Operational Readiness Review (ORR) scheduled for the end of March, 2010. Further details of the MMOC are provided in the technical section of this proposal.

In conclusion, *Wind* is operationally healthy and continues to maintain a large fuel reserve, capable of sustaining the spacecraft at L1 for almost 60 years.

1.3 Unique Capabilities of *Wind*

Wind's complement of instruments was optimized for studies of solar wind plasma, interplanetary magnetic field, radio and plasma waves, and of low energetic particles. It is by no means equivalent to that on ACE. Rather, the two missions, by design, are very complementary. ACE - launched a few years after *Wind* - focuses on the detailed investigation of high energy particles for which *Wind* has limited capabilities. Therefore, several of the *Wind* solar wind, suprathermal particle, and especially radio and plasma wave instruments are unique. The *Wind* instrument capabilities are summarized in Table 1 and compared to ACE and STEREO. ***For solar wind, low energy particle and radio waves observations, Wind is the only near-Earth spacecraft that can match those provided by STEREO.*** A more detailed discussion of the unique *Wind* capabilities follows in the next paragraphs.

Collaborating with STEREO, *Wind/WAVES* provides an essential third vantage point along the Sun-Earth line, allowing the unambiguous localization of inner heliospheric radio sources and the determination of their corresponding beam patterns. Moreover, the WAVES frequency coverage extends to the thermal noise regime, where it provides an independent measurement of the solar wind electron plasma frequency. This quantity is directly proportional to the square root of the solar wind electron plasma density. Thus the density, normally obtained as a moment or fit of the distribution function from SWE and 3DP, can also be accurately and independently derived from the WAVES instrument and used to re-

Table 1. The measurement capabilities of *Wind* compared to STEREO and ACE. The table illustrates the complementarity of *Wind* and ACE. While at high energies ACE clearly dominates, for the thermal plasma, low energy particles and radio waves *Wind* is the only near-Earth spacecraft providing measurements that can match those obtained by STEREO.

Measurement	Wind	STEREO	ACE	Comments for Wind
DC Magntic Field	MFI 1/22 sec	MAG 1/8 sec	MAG 1 sec	Highest time resolution measurements
Radio and Plasma Waves	WAVES 4kHz-14MHz	SWAVES 10kHz-16MHz		Low frequency measurements to obtain \bar{n} density
Solar Wind Ions	3DP moments: 3sec distr.: 24sec burst: 3sec SWE moments:92sec	PLASTIC moments: 1min	SWEPAM moments: 64s	Highest time resolution observations Robust and redundant observations under solar storm conditions
Solar Wind Electrons	3DP - 3 sec SWE - 9 sec	SWEA 2 sec	SWEPAM 128 sec	High time resolution observations
Solar Wind Composition	SMS/STICS $1 \leq Z \leq 56$ 8-230 keV/Q	PLASTIC $1 \leq Z \leq 56$ $\sim 0.3-80$ keV/Q	SWICS $1 \leq Z \leq 30$ 0.5-100 keV/Q	Unique observations for the >100 keV/Q range
Solar Wind Mass Spectrometry	SMS/MASS $2 \leq Z \leq 28$ 0.5-12 keV/Q		SWIMS $2 \leq Z \leq 30$ 0.5-20 keV/Q	Comparable to ACE observations
Low Energy Electrons	3DP $\sim 0 - 400$ keV	STE $\sim 0 - 100$ keV	SWEPAM $\sim 0 - 1.35$ keV	Unique coverage of electrons up to 400 keV
Low Energy Ions	3DP 3 eV-11 MeV	SEP/SEPT 60 keV-7 MeV	ULEIS 20 keV-14 MeV	Comparable observations
High Energy Particles	EPACT/LEMT 40 keV - 50 MeV/nuc	SEP 30 keV - 100 MeV/nuc	ULEIS/SIS 20 keV - 167 MeV/nuc	Robust, high geometrical factor directional observations

fine the calibration of the plasma instruments.

The *Wind*/3DP instrument detects solar energetic particle events, in particular, impulsive electron events, from ~ 1 keV (sometimes ~ 0.1 keV) to ~ 400 keV. Electrons in this energy range produce most of the flare hard X-rays detected and imaged by RHESI (>3 keV). *No instrument on any other spacecraft has the high sensitivity required for solar/heliospheric electron measurements from a few to 40 keV.* In addition, the *Wind* electron measurements from 40 keV to ~ 400 keV are the most sensitive of any instrument currently operating, and only 3DP provides full 3D measurements. These are crucial measurements because solar electrons from ~ 0.1 to ~ 100 keV are excellent tracers of the structure and topology of interplanetary magnetic field lines. Fi-

nally, the 3DP 3-second high time resolution plasma observations are unequaled by any other spacecraft and are essential for microphysics studies.

With 3DP and SWE, Wind is the only spacecraft capable of measuring full 3D distributions of ions and electrons continuously from thermal plasma to MeV energies. A unique capability of the SWE Faraday Cup is its accuracy and stability even during large solar storm events when other instrument types have difficulty making measurements.

Wind also carries unique solar wind composition instruments. Currently, the STICS sensor, in the *Wind*/SMS suite, provides the only measurements at 1AU of ion composition up to 200 keV/q.

Because of its great dynamic range, *Wind*'s energetic particle instrument (EPACT) has a proven

capability of measuring solar energetic particles (SEPs) during particularly enhanced solar storm conditions without the inherent saturation problems of other instruments. The EPACT Low Energy Matrix Telescopes (LEMTs) cover an energy range for observing elemental abundances of SEPs that is just between that of ULEIS and SIS (both on ACE). The EPACT/STEP instrument on *Wind*, although it does not have the isotopic resolution of ULEIS, does have comparable sensitivity and fast on-board identification of elements from He to above Fe. LEMT has a very large collection power and identifies particle species and incident energy on-board at rates up to tens of thousands of particles per second. This permits the observation of temporal variations in elemental abundances on short time scales. Finally, due to *Wind*'s spin within the ecliptic plane and because of the instruments' large field-of-view, EPACT provides comprehensive SEP ion anisotropy measurements that are unavailable from any other spacecraft.

1.4 Heliophysics Great Observatory

Wind plays an active role in the Heliophysics Great Observatory (HGO). *Wind* achieved many of its recent scientific discoveries in collaboration with other spacecraft as described in more detail in the Science Accomplishments section below. However, the HGO is more than just the occasional comparison of data from multiple platforms. It is a data environment where such comparisons can be readily performed. As the Heliophysics Data Policy outlines, this data environment requires the presence of in-depth metadata for each data product based on a uniform standard (the SPASE dictionary). It also envisions the eventual connection of the current distributed data repositories by a number of virtual observatories enabling the location and downloading of the desired data. *Wind* plays a leadership role in the deployment of the Virtual Heliospheric Observatory (VHO), the heliospheric portion of this environment, and the generation of the corresponding metadata. Even though the VHO is not yet fully deployed, almost all *Wind* instruments already have VHO compliant data services. It is expected that by the delivery date of the first complete VHO (no more than two years from now), more *Wind* data with more description will be available through VHO than via traditional means. Moreover, since *Wind* has many well developed software libraries, *Wind* teams will

also lead in the next phase of data environment development: customizable data services.

1.5 Living With a Star Program

The Living With a Star (LWS) program seeks to better understand the Sun-Earth connected system with the aim of developing reliable space weather forecasting capabilities. The program architecture plan calls for a near-Earth solar wind monitor to connect the solar (SDO) and inner heliospheric (*Solar Probe+*, *Solar Orbiter* and *Sentinels*) observations with geomagnetic ones (RBSP). However, NASA has no current plans for a new solar wind monitoring mission, rather NASA assumes that *Wind*, ACE or both will survive into the 2012-2022 time frame. Because both *Wind* and ACE are well past their prime missions and design lifetimes, the lowest risk option to satisfy the near-Earth solar wind monitoring requirement of LWS is to sustain both *Wind* and ACE, either of which can satisfy the LWS measurement requirements. Though we again point out that *Wind* and ACE are not duplicate spacecraft but rather serve complementary roles. Thus, the most prudent course of action involves preserving both spacecraft.

2. SCIENCE ACCOMPLISHMENTS AND GOALS

Two of the great unanswered questions of heliophysics are what heats the corona and accelerates the solar wind and what are the physical processes that produce Solar Energetic Particles (SEPs). Three upcoming missions are dedicated to resolving these outstanding issues: *Solar Probe+*, *Solar Orbiter* and LWS *Sentinels*. All of these new missions will head to the inner heliosphere where their observations will be significantly limited by telemetry constraints and by the large solar heat flux that makes sunward pointed particle telescopes difficult to operate. However, the solar wind carries to 1 AU telltale signs of its origin and of the critical processes that accelerate particles. Thus the uniquely high time resolution and 4π , full sky comprehensive fields and particles observations of *Wind* have resulted in a steady stream of discoveries during the past years constraining solar wind and SEP theories and models. In collaboration with STEREO and ACE, *Wind* has also significantly contributed to our understanding of ICME structure and the global properties of the heliosphere during the current unusually long solar minimum. Finally,

Wind remains a critical source of solar wind input for Earth magnetospheric studies. In this section, we highlight recent *Wind* discoveries organizing them along the three heliophysics research objective areas. Moreover, we demonstrate that as a result of newly developed theories and models, and due to improved instrument data production and analysis, *Wind* will continue to contribute significantly to new discoveries and understanding of the origin and structure of the solar wind and of the acceleration and modulation of SEPs. Our detailed science plans for the 2011-2014 period are outlined at the end of each science subsection.

2.1 HELIOPHYSICS OBJECTIVE #1: Fundamental Physical Processes

The first heliophysics research objective, as articulated by the *Science Plan for NASA's Science Mission Directorate 2007-2016*, is to understand the fundamental physical processes of the space environment from the Sun to Earth. *Wind* observations were key to making progress in two of the focus areas of this objective: (1) understanding the plasma processes that accelerate and transport both the solar wind and energetic particles; and (2) understanding magnetic reconnection.

2.1.1 Understanding the origin and acceleration of the solar wind

Even fifty years after the supersonically expanding solar wind was discovered, the fundamentals of how the extended corona of the Sun is heated and accelerated remain unknown. Current theories on how energy is flowing from the solar surface to the corona rely on various forms of collisional coupling or on the dissipation of large amplitude Alfvén waves and turbulence that result in particle heating [e.g., *Verdini and Velli, 2007*]. Even though most of the solar wind acceleration takes place within a few solar radii from the Sun, many signatures of the physical processes at work remain detectable at 1 AU. *Wind* has made significant progress identifying these signatures.

(1) Solar wind Helium temperature anisotropy

Solar wind acceleration models of wave dissipation through resonant scattering postulate that waves couple to heavier ions depending on their mass, charge and relative speeds increasing their temperatures. These models inherently require a multi-fluid,

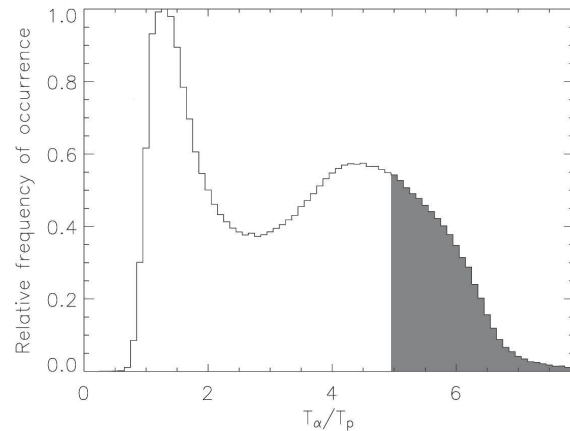


Figure 2. The relative occurrence of the alpha over proton temperature ratio, T_{α}/T_p in the solar wind over the course of the *Wind* mission, illustrating the bimodal nature of the dominant components of the plasma. For 23% of the observations $T_{\alpha}/T_p > 5$, indicating anomalous heating beyond the already unusual equilibration of thermal speeds. [*Kasper et al., 2008*].

anisotropic description of the solar wind plasma [e.g., *Hernandez et al., 1987; Cranmer et al., 1999*]. After many years of development, the *Wind* Solar Wind Experiment (SWE) team was able to determine not only the independent solar wind proton and alpha temperatures but also their anisotropies fitting separate bi-Maxwellian distributions to the proton and alpha peaks [*Kasper et al., 2006, 2007*]. Figure 2 shows the occurrence rate of the various values of alpha over proton temperatures collected through the entire mission. Strict temperature equilibrium required by a single-fluid plasma description would yield a ratio of 1. While the observations clearly peak at this value, there is a significant secondary peak that violates energy equipartition. Moreover T_{α}/T_p values over 5 (shaded gray) imply a heating mechanism that couples to individual particles rather than to the whole solar wind ensemble. One such mechanism involves large amplitude Alfvén waves in the core proton population propagating outward from the Sun and coming into cyclotron resonance with the various minor ions (such as alpha particles). This resonance transfers energy from the wave to the minor ions preferentially heating the particles perpendicular to the local magnetic field. This process is only efficient if the minor ions, that tend to travel faster than the protons, slow down to nearly the speed of protons. *Kasper et al. [2008]*, using the newly processed *Wind* proton and alpha data, has

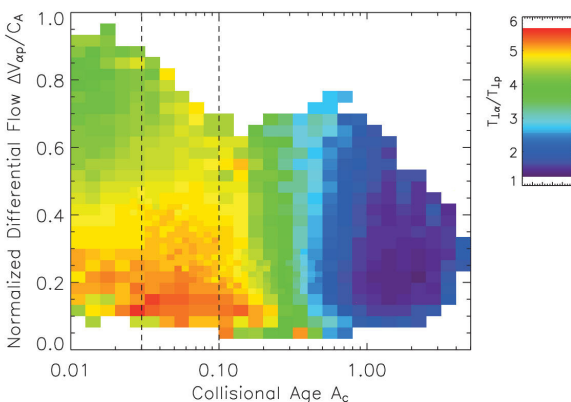


Figure 3. The ratio of the perpendicular component of the ion temperatures as a function of the collisional age A_c and $\Delta V_{\perp}/C_A$, the differential flow between the two species normalized by the local Alfvén speed. [Kasper *et al.*, 2008]

shown that indeed the perpendicular temperature of the alphas are significantly enhanced for collisionally young parcels of solar wind when their differential flow is very small (see Figure 3). This seminal result provides experimental evidence at 1 AU for a particular wave dissipation solar wind acceleration theory. The significance of this work was recognized in a featured Viewpoint article in Physical Review Letters [Bale, 2008].

(2) Non-Thermal Solar Wind distributions

Another signature of the processes accelerating the solar wind plasma is the frequent non-Maxwellian features of the thermal ion velocity distribution functions [e.g., Tu *et al.*, 2004; Goldstein *et al.*, 2000]. In particular, a secondary proton beam, well separated in velocity from the core, is pervasive in the fast solar wind, which is collisionally young [Marsch *et al.*, 1982]. It is occasionally also observed in the slow solar wind [Marsch, 2006]. The beam is characterized by a differential flow on the order of the Alfvén speed relative to the core, oriented along the local magnetic field direction. Recently, Stevens *et al.* [2009] developed a new technique that allows the nonlinear fitting of multiple proton and alpha components of the *Wind* Faraday Cup observations. Applying this technique to the 15 years of *Wind* observations, they have found a secondary proton beam of Alfvénic nature in about one percent of cases, and a non-Alfvénic, warm second component in four percent of all spectra (see Figure 4). These non-thermal structures are clear fingerprints of kinetic processes that accelerate the solar wind, but

their exact origin and nature is not well understood at this time. This new *Wind* Faraday Cup fitting process and large data set allows the characterization of these secondary populations as a function of the various solar wind properties constraining the theoretical models that seek to explain their presence.

(3) Wave-Particle Interactions in the Expanding Solar Wind

After the initial acceleration of the solar wind to super-Alfvénic speeds, the physical processes that regulate the expansion of this plasma include adiabatic particle motion, plasma instabilities and binary particle collisions. As the solar wind streams away from the Sun, it expands decreasing the plasma density and magnetic field magnitude. The plasma temperature perpendicular to the magnetic field would also be expected to drop, with the parallel component staying nearly constant, leading to extremely large temperature anisotropies. This, however, is not observed at 1 AU and beyond. Theory predicts that Coulomb collisions and pressure-anisotropy instabilities act to pitch-angle scatter the plasma back towards isotropy [Eviatar and Schultz, 1970]. Using over a million independent measurements of

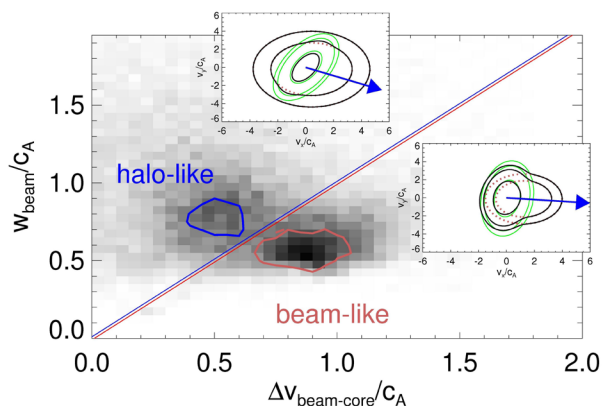


Figure 4. A 2D histogram of secondary ion components from the new *Wind* Faraday Cup fits. The density of points is plotted as a function of the differential and thermal speeds, normalized to the local Alfvén speed. The distribution is clearly bimodal. Spectra near the slow and hot peak are considered halo-like, and the spectra near the cold and fast one are beam-like. Overlaid are two examples of the new, multi-component distribution functions (black contours). The original, single component fit results are shown in green. Red dashes identify the secondary component alone and the blue arrows indicate the concurrent magnetic field direction. [Stevens *et al.*, 2009]

the solar wind proton temperature anisotropy and gyroscale magnetic fluctuations detected by *Wind*, *Bale et al.* [2009], showed for the first time observationally that magnetic fluctuations are indeed enhanced along the temperature anisotropy threshold of the mirror, proton oblique firehose and ion cyclotron instabilities. These enhanced magnetic fluctuations serve to redistribute energy in the solar wind and maintain an isotropic distribution. This explains how the non-collisional thermal solar wind can possess an isotropic distribution function, normally a hallmark of collisional gases. This observational result is key to understanding the evolution of the solar wind from near the Sun to 1 AU and beyond.

Future Plans:

A number of new *Wind* data products (such as separate alpha and multi-component proton beam fits) that will enable further research into the origin and acceleration of the solar wind became publicly available recently. In addition, the newly recalibrated SWE electron and 11 vector/second magnetic field data provides the necessary high time resolution measurements required to investigate wave-particle interactions and wave dissipation mechanisms. Furthermore, we are in the process of developing a standardized format for the description of particle distribution functions. This will enable the wider scientific community to have easy access to the kinetic description of the solar wind plasma.

2.1.2 Understanding reconnection in the solar wind

Besides dissipation of large amplitude Alfvén waves, particle collisions and turbulence, magnetic reconnection in the form of nano-flares is the most likely mechanism to heat the solar corona. While the nano-flares clearly take place low in the corona, the same physical mechanism can be studied at 1 AU in the solar wind [*Gosling et al.*, 2005]. The high time resolution *Wind* thermal plasma and magnetic field observations have been particularly critical in making progress in this field.

(1) The physics of low-shear reconnection in the solar wind

One of the telltale signs of reconnection in the solar wind is a reconnection exhaust that is embedded in the solar wind flow and is convected past a spacecraft on a variety of time scales. Multi-spacecraft observations revealed extremely long reconnection

X-lines at 1 AU extending hundreds of Earth radii [*Phan et al.*, 2006; *Gosling et al.*, 2007a, b; *Phan et al.*, 2009]. However, all extended X-line events reported so far were found in large ($>70^\circ$) magnetic shear current sheets where the reconnection exhausts are wide. Reconnection models predict that, closer to the Sun, strong guide-field, low-shear reconnection events dominate. Recent high time resolution *Wind* observations led to the discovery that even at 1 AU low magnetic shear (thus much narrower) reconnection exhausts are far more common than the wider, high shear ones [*Gosling et al.*, 2007c; *Gosling and Szabo*, 2008]. This discovery allows us to start studying this critical solar wind heating mechanism even before the launch of the *Solar Probe+* mission.

(2) Local characteristics of reconnection exhausts

The *Wind* high time resolution observations also led to a number of discoveries concerning the nature and characteristics of the reconnection exhaust itself. Multiple reconnection exhausts were observed within magnetic clouds, including some at very small ($< 15^\circ$) local field shear angles, and apparently bifurcated current sheets (a common signature of a reconnection exhaust) on spatial and temporal scales too small to be resolved even by the 3-second *Wind* plasma measurement but visible by the 11 vectors/second *Wind* magnetic field observations [*Gosling and Szabo*, 2008]. *Eriksson et al.* [2009] have found flow shear effects on top of the magnetic signatures of the exhausts on opposite sides of a reconnection X-line, and *Lavraud et al.* [2009] identified suprathermal electron signatures of an extended separatrix region in an exhaust observed on the sunward side of the heliospheric current sheet. Moreover, *Wind* observations were also key in the understanding of the prevalence of extended reconnection X-lines in the solar wind and the near planarity of virtually all reconnection exhaust boundaries [*Phan et al.*, 2009].

(3) Electron acceleration near the Sun due to reconnection

Besides directly observing reconnection events at 1 AU, *Wind* also allows the remote observation of coronal reconnections by measuring the accelerated particles. Comparison of *Wind* measurements of energetic electrons in solar impulsive events with the electrons producing the flare hard X-ray emissions at the Sun observed by RHESSI provides unique

information on the energetic electron acceleration and escape processes. For prompt events (where the injection of the electrons at the Sun, inferred from their velocity dispersion, is simultaneous with the X-ray bursts) a close correlation was found between the power-law exponents of the spectra of the electrons at 1 AU and those of the X-ray producing electrons. For delayed events, however, this correlation does not exist. This suggests a common source for the flare-accelerated electrons and the escaping electrons for prompt events, and likely two different electron populations for the delayed events [Krucker *et al.*, 2007]. For prompt events, RHESSI's X-ray imaging together with TRACE imaging of lower temperature plasmas show accompanying jets consistent with reconnection of an open field line with a closed loop (inter-change reconnection). However, for the same prompt events, a simple model, where the electrons observed at 1 AU escape directly from the acceleration source while the downward going accelerated electrons produce the X-rays while losing all their energy to collisions in the dense lower solar atmosphere ('thick target model'), does not fit. Some additional acceleration of the downward-propagating electrons may be occurring. If magnetic reconnection does the initial acceleration, the downward-propagating electrons are possibly further accelerated by Fermi and betatron processes as the newly closed field line becomes more dipolar. Another possible explanation of the observed spectral correlation is re-acceleration where a rather faint electron beam accelerated in the corona acts as the seed population for a second acceleration occurring in the chromospheric footpoints [Brown *et al.*, 2009].

(4) *Periodic solar wind density fluctuations*

Even the thermal solar wind ions carry possible signatures of coronal reconnection. In a recent study using 11 years of solar wind observations from the *Wind* spacecraft, Viall *et al.*, [2008] showed that periodic proton density structures occurred with preferred wave-lengths. During these intervals of significant periodic density fluctuations, the solar wind velocity remained relatively steady while the magnetic field variations broadly maintained the structures in pressure balance, suggesting that these were static, convecting structures rather than propagating waves [Kepko *et al.*, 2002; Kepko and Spence, 2003]. Further analysis of the alpha and proton

abundance ratio revealed a strong anti-correlation between these two solar wind components [Viall *et al.*, 2009]. Since the composition of the solar wind cannot be easily modified during transit, this result implies a coronal origin for these fluctuations. One possible explanation is that the density variations are signatures of periodic reconnection at the tip of helmet streamers releasing solar wind parcels with the alpha component gravitationally settling and thus being delayed compared to the proton streams. [Endeve *et al.*, 2005].

Future Plans:

Because of the high temporal cadence of the *Wind* plasma measurements, the *Wind* observations will play a central role in almost all studies of reconnection as it occurs in the solar wind for the foreseeable future, including long-term studies associated with the advance of the solar activity cycle. The solar wind measurements are particularly important since they provide a unique laboratory to study details of the overall reconnection process on spatial and temporal scales unavailable anywhere else. In particular, the newly developed multi-beam proton fitting of the *Wind*/SWE data providing non-Maxwellian distributions that contain the fingerprints of heating processes in the solar wind and in the corona, will allow the detailed investigation of reconnection exhausts. Counter-streaming protons can provide in-situ evidence of plasma interpenetration at magnetic reconnection exhaust sites, yielding insight into the flow diversion mechanism in those structures. During the rising phase of the new solar cycle, it is expected that the rate of observed reconnection events will significantly increase enabling the detailed study of this critical physical process.

2.1.3 Understanding the acceleration and transport of solar energetic particles

The acceleration of solar energetic particles is also not a well understood phenomenon. Collisionless shock waves are a topic of considerable relevance due to their ability to efficiently heat and/or accelerate charged particles via energy dissipation. Proposed energy dissipation mechanisms include wave dispersion [Mellott and Greenstadt, 1984], particle reflection [Edmiston and Kennel, 1984; Kennel, 1987], and anomalous resistivity due to wave-particle interactions [Gary, 1981]. However, the relative importance of the various mechanisms

is still a matter of debate. Because of its excellent quality of combined field and plasma measurements, *Wind* remains an invaluable tool for the study of shock physics.

(1) Wave-particle interactions at interplanetary shocks

Recent observations of interplanetary (IP) shocks using *Wind* data [Wilson III et al., 2007, 2009, 2010] have found new evidence of the importance of wave-particle interactions. The *Wind* Time Domain Sampler (TDS), a part of the *Wind*/WAVES investigation, was the first instrument capable of resolving the waveforms of high frequency (≥ 1 kHz) waves in the solar wind. Data from this instrument allowed Wilson III et al. [2007] to discover a correlation between large amplitude (≥ 5 mV/m peak-to-peak) ion-acoustic waves (IAWs) and the Mach number and compression ratio of IP shocks, consistent with the generation of large cross-field currents that provide free energy for wave generation. Quasi-linear estimates of the anomalous resistivities produced by these large amplitude IAWs range from ~ 1 -856 Ωm

($\sim 10^7$ times greater than classical estimates), but two to three orders of magnitude below Vlasov simulation estimates using realistic mass ratios [Petkaki et al., 2006].

Wind also provides full 4π steradian electron and ion distribution coverage with 3-second time resolution, a capability still unrivaled among dedicated solar wind missions. These high cadence particle distributions (see Figure 5), in combination with high cadence magnetic field measurements from the fluxgate magnetometer, allow *Wind* to examine the microphysics of low frequency (≤ 10 Hz) structures in the solar wind. Wilson III et al. [2009], in a study of low frequency ($0.25 \text{ Hz} < f < 10 \text{ Hz}$) waves at five IP shocks, found that the multi-component nature of the solar wind electron distribution function may be more important than previously thought, consistent with new theories on wave-particle interactions between solar wind electrons and whistler mode waves [Saito and Gary, 2007]. They also observed whistler mode waves simultaneously with electron distributions unstable to an anisotropy and/or heat flux in-

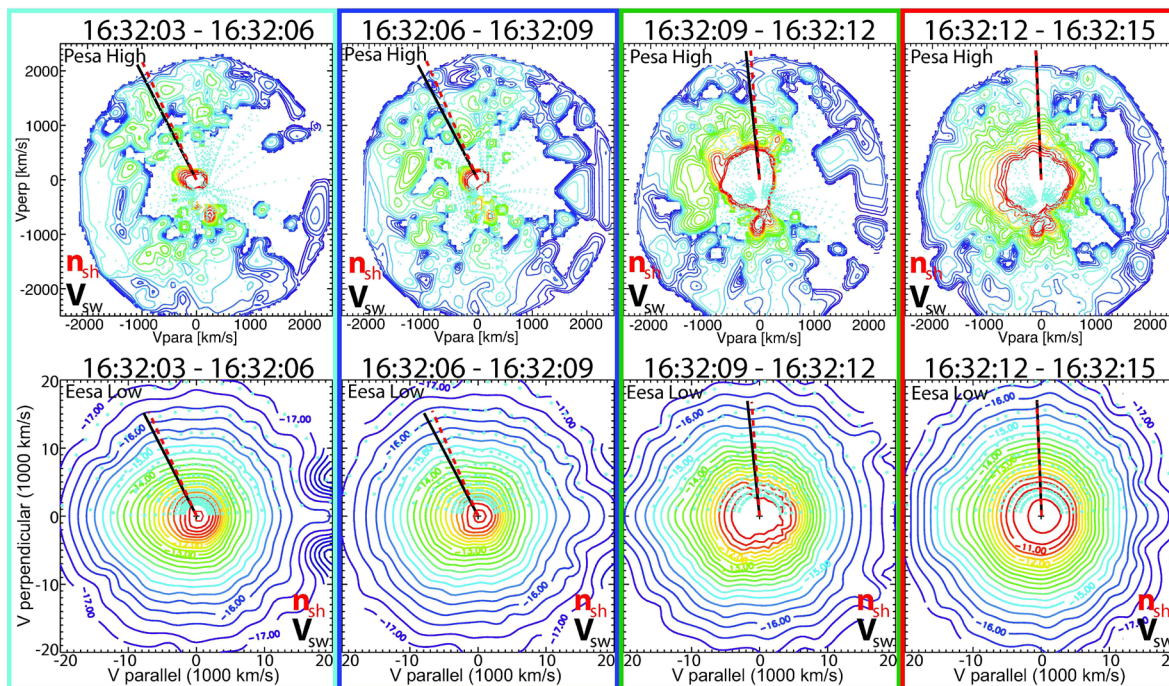


Figure 5. Four particle distributions for protons (top) and electrons (bottom) obtained by the *Wind* 3DP instrument across an interplanetary shock with a rapid 3 second cadence. The horizontal axis of each plot is parallel to the magnetic field and the vertical axis is perpendicular in the plane created by the solar wind velocity and magnetic field direction. The black solid line represents the projection of the solar wind velocity and the red dotted line represents the shock normal vector projection. The figure illustrates strong anisotropic particle heating in both the ions and electrons beyond the adiabatic limit. The heating is associated with large amplitude waves at an IP shock, simultaneous measurements only the *Wind* spacecraft is capable of making in the solar wind. [Wilson III et al., 2010].

stability, supporting the suggestion of *Gary et al.* [1994, 1999] that halo electrons are more important for the excitation of whistler waves than the core. The unique array of high cadence particle and field measurements on *Wind* make it an essential element in the study of wave-particle interactions in the solar wind. Even though at 1 AU the observed particle heating is relatively small, the same mechanisms closer to the Sun are believed to be responsible for the acceleration of energetic particles.

(2) Origin and propagation of solar electron/³He-rich event

Impulsive SEP events are dominated by ~ 1 -100 keV electrons (high electron-to-proton ratios) and low-energy, ~ 0.01 to ~ 10 MeV/nucleon ion emissions with small particle intensities, enhanced ³He/⁴He ratios up to 10^4 times the coronal values, and high heavy-ion ionization states [*Mason, 2007*], and are often associated with an impulsive soft X-ray (SXR) burst. These impulsive events - also called “electron/³He-rich SEP events” - are the most common impulsive solar particle acceleration phenomena. *Wind*/3DP observations were used to carry out the first comprehensive study of these solar impulsive electron events (Wang L., PhD thesis 2009). In this study, 1191 solar electron events were detected from 1995 through 2005 [*Wang et al., 2010a*] showing a strong solar-cycle variation. These solar energetic electron events have a one-to-one association with Type III radio bursts and a close ($\sim 78\%$) association with low-energy, ³He-rich ion emissions, but a poor association with GOES SXR flares.

The case studies of the timing of nearly scatter-free electron/³He-rich SEP events with good count statistics [*Wang et al., 2006; 2010b*] suggest that at the Sun, the low-energy (~ 0.4 to 6 - 9 keV) electron injection starts ~ 9 min before the coronal release of the Type III radio burst; the high-energy (~ 13 to ~ 300 keV) electron injection starts ~ 8 min after the Type III burst; and the injection of \sim MeV/nucleon, ³He-rich ions begins ~ 1 hour later (Figure 6). The selected electron/³He-rich SEP events also have a remarkable one-to-one association with fast west-limb narrow CMEs. A case study of the electron propagation in solar impulsive electron events [*Wang et al., 2010c*] suggests that low-energy (≤ 10 - 30 keV) and high-energy (≥ 10 - 30 keV) electrons propagate differently in the interplanetary medium, with more scattering at high energies. Such scatter-

ing appears to be caused by resonance with waves/turbulence at scales greater than the thermal proton gyroradius in the solar wind. Although the transition to more scattering occurs at energies where the electron injection delays are detected, the scattering is not enough to produce these delays.

Based on these *Wind* results, a coherent picture of electron/³He-rich SEP events can be built up. At the Sun, the low-energy (~ 0.4 to 6 - 9 keV) electrons may be accelerated in jets that are ejected upward from magnetic reconnection sites between closed and open field lines. These low-energy electrons then generate the Type III radio bursts. The jets may appear as CMEs high in the corona, and the high-energy (~ 13 to ~ 300 keV) electrons may then be accelerated at $\geq 1 R_s$ by CMEs, acting on the seed electrons provided by the low-energy injection. The ~ 1 MeV/nucleon, ³He-rich ions may be accelerated by selective resonance with electron-beam generated waves and/or by fast, narrow CMEs. In the interplanetary medium, both low and high energy electrons often propagate nearly scatter-free, but the high-energy electrons experience more scattering than the low-energy electrons, likely by waves/turbulence generated by solar wind ions.

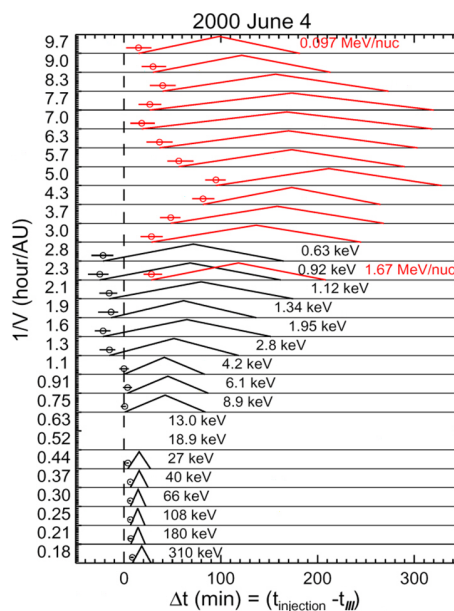


Figure 6. Inferred solar injection profiles of electrons (black) and ions (red) for the 4 June 2000 event. The X-axis shows the time in minutes, with respect to the release time of Type III radio burst at the Sun (dash line). The Y-axis shows the energy in terms of $1/\text{speed}$. The circles indicate the start-time of particle injections. [*Wang et al., 2010c*]

(3) *The source region and compositional variability of solar energetic particles*

Besides understanding the acceleration and propagation of energetic electrons, *Wind* has also significantly contributed to the subject of solar energetic ion origin and transport. In a recent study based on 12 gradual solar energetic particle events observed by both *Wind* and ACE, *Ko et al.* [2010] examined the correlation between their source regions and heavy-ion composition. They found that the SEP elemental composition at ~ 0.1 -10 MeV/nucleon falls into two classes, depending on whether the associated solar wind, and correspondingly the footpoint of the magnetic field along which the SEPs are transported, is from an active region or from a coronal hole. Specifically, the observed SEP Fe/O ratio is preferentially enhanced in the case of active region footpoints (see Figure 7). Events with lower than average SEP C/O are also preferentially associated with active region footpoints. By contrast, the distributions of Fe/O and C/O for the in-situ solar wind thermal particles in these time intervals are essentially indistinguishable. These results are the first successful examples of tracking SEP event-to-event compositional variation back to differences in the solar source regions. These results open a new window onto understanding the origin of SEPs, their acceleration and transport.

(4) *The source regions of Ground Level Event (GLE) particles*

Ground Level Events (GLEs) are the largest solar energetic particle events with sufficiently hard spectra for GeV protons to be detected by neutron monitors at ground level. Relying on the large collecting power of the *Wind*/EPACT/LEMT instrument, *Reames* [2009] has performed a velocity dispersion analysis that yielded the initial solar particle release (SPR) time and the magnetic path length traveled for the largest GLE events. He has found that for a given GLE, all particle species and energies diverge from a single SPR point at a given coronal height and footpoint longitude of the field line to the Earth. These heights tend to increase with longitudinal distance away from the source, a pattern expected for shock acceleration. Acceleration for magnetically well-connected large GLEs begins at ~ 2 solar radii, in contrast to lower energy non-GLEs that have been found to be strongly associated with shocks above ~ 3 solar radii. The higher densities and magnetic field strengths at lower altitudes may be responsible for the acceleration of the higher-energy particles in GLEs, while those GLEs that begin above 3 solar radii may compensate by having higher shock speeds. These results support the joint dependence of maximum particle energy on magnetic field strength, injected particle density,

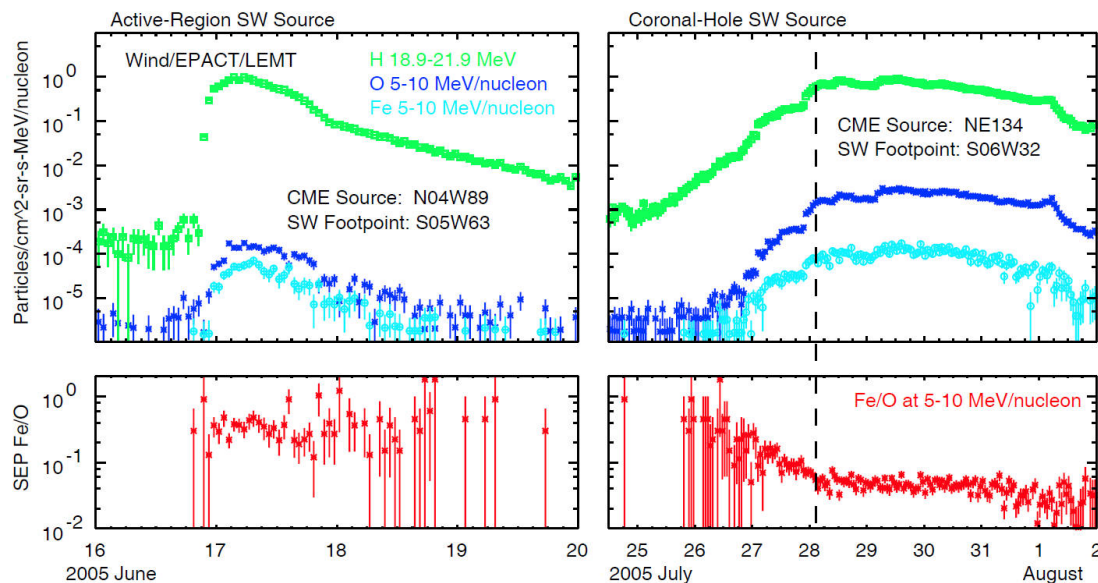


Figure 7. The time histories of SEP proton, Fe and O intensity (top) and Fe/O ratios (bottom) from *Wind*/EPACT/LEMT for a gradual SEP event in which the magnetic field traces back to a footpoint near an AR (left) or a CH (right). The dashed vertical line in the right panel marks the transition from one CH field-line footpoint to another. [*Ko et al.*, 2010]

and shock speed, all predicted theoretically.

Future Plans:

The continued operation of *Wind* will enable many new studies investigating the process of particle acceleration in the inner heliosphere besides the continuation of the above outlined research. Combining *Wind*, ACE and STEREO, together with ICME modeling, will map quasi-parallel and quasi-perpendicular regions around ICME-driven shocks to interplanetary SEP abundance and spectral observations at different spacecraft locations. The resulting correlations will quantitatively limit which acceleration theories are viable.

We will also combine the *Wind*/3DP and STEREO/STE data measured during November 2006 - January 2007, when the two spacecraft were at similar locations, to construct high-resolution 3-dimensional distributions of interplanetary suprathermal electrons. Furthermore, we will also compare the *Wind*/3DP and STEREO/STE measurements made since January 2007, when the three spacecraft moved significantly apart, to examine the spatial variation of interplanetary suprathermal electrons, and thus gain a better understanding of their acceleration process. Moreover, combining RHESSI observations of energetic electron source regions with in situ electron measurements will allow the determination of the precise beam widths of the electron radiation and constrain theories for their acceleration.

Finally, closer inspection of a supercritical shock from the *Wilson III et al.* [2009] study has revealed anisotropic particle heating and signatures of electron cyclotron drift instability driven waves [*Wilson III et al.*, 2010]. Both the core and halo ion and electron distributions were heated beyond the adiabatic limit. Further investigation and identification of different wave modes and their effects on the plasma will provide a more complete accounting of the energy budget of IP shocks and thus an insight into the acceleration process of energetic particles at shocks.

2.2 HELIOPHYSICS OBJECTIVE #2: Evolution of Solar Transients in the Heliosphere

The second heliospheric research objective, as described by the *Science Plan for NASA's Science Mission Directorate 2007-2016*, focuses on how the heliospheric manifestations of solar activity evolve

before reaching Earth and how they affect the magnetosphere. The Sun's output varies on many time scales. *Wind*'s high time resolution, stable and reliable measurements carried out over 15 years (more than a solar cycle) have significantly contributed to studies of solar wind structures on all scale-lengths ranging from turbulent energy cascade to the structure and propagation of interplanetary coronal mass ejections (ICMEs). This section highlights some of the outstanding *Wind* results from this area with our future plans again detailed at the end of each subsection.

2.2.1 The long and quiet solar minimum

The declining phase of the last solar cycle (Cycle 23) and the ensuing solar minimum were unusually long and quiet. While this significantly limited the number of transients that could be studied, the resulting steady solar wind configuration provided an excellent opportunity to investigate the global structure of the inner heliosphere. Moreover, the over 15 years of *Wind* observations with the extremely stable SWE Faraday Cup and MFI magnetometer instruments allowed the detailed comparison of the current unusual solar minimum to the previous one.

(1) Solar wind Quasi-Invariant as a proxy for solar activity

Previous studies have found that the ratio of the solar wind magnetic energy density to the plasma kinetic energy density (i.e., the inverse square of the Alfvén Mach number), is a good proxy for solar activity, correlating very well with the solar sunspot number at various heliospheric distances. It has thus been called a “quasi-invariant” (QI) [*Osherovich, et al.*, 1999]. It has the advantage of being a quantity that is locally determined from in-situ solar wind measurements and thus can function as a heliospheric index of solar activity. Using STEREO and *Wind* plasma and magnetic field data, *Leitner et al.*, [2009] compared the distribution of the QI during the last and current solar minima and found the current values significantly depressed. They fitted the QI distributions with both log-normal and log-kappa distributions and found a better match with the latter [*Leitner et al.*, 2010]. The newly fitted log-kappa distributions allow the detailed comparison of previous solar minima.

(2) Stronger and longer high-speed streams during this solar minimum

Even though the present solar minimum is exceptionally quiet, with sunspot numbers at their lowest in 75 years and the solar wind magnetic field strength lower than ever observed, the solar wind still has a very prominent structure that strongly impacts the Earth's magnetosphere. Despite, or perhaps because of, a global weakness in the heliospheric magnetic field, large near-equatorial coronal holes have lingered even as the sunspots disappeared. Consequently, *Wind* has recorded strong, long and recurring high-speed streams impinging on the Earth's magnetosphere in contrast to the weaker and more sporadic streams that *Wind* observed during the last solar minimum (see Figure 8) [Gibson, et al., 2009]. In response, geospace and upper atmospheric parameters continued to ring with the periodicities of the solar wind in a manner that was absent last cycle minimum, and the flux of relativistic electrons in the Earth's outer radiation belt was elevated to levels more than three times higher than eleven years before. These large high-speed streams were very stable and could be positively identified even in the longitudinally well separated STEREO observations [Luhmann et al., 2009]. These results point out that

the geoeffectiveness of the quiet solar wind cannot be accurately predicted by the sunspot numbers alone but require in-situ heliospheric observations, such as provided by *Wind*.

Future Plans:

During the 2013-2017 time frame, the solar cycle will be in its rising phase with the structure of the inner heliosphere rapidly becoming more complex. By November 2016, *Wind* will complete 22 years of continuous solar wind observations (a complete 22-year solar cycle). *Wind's* reliable and steady solar wind instrumentation, will allow the detailed comparison of three separate solar cycle rising phases and the determination as to whether or not Cycle 24 continues to be a highly unusual solar cycle.

2.2.2 Interplanetary Coronal Mass Ejections (ICMEs) and their driven shocks

ICMEs are the most significant mechanism for injecting new magnetic flux into the heliosphere. Also many ICMEs, with strong and steady southward fields, are the primary causes of geomagnetic

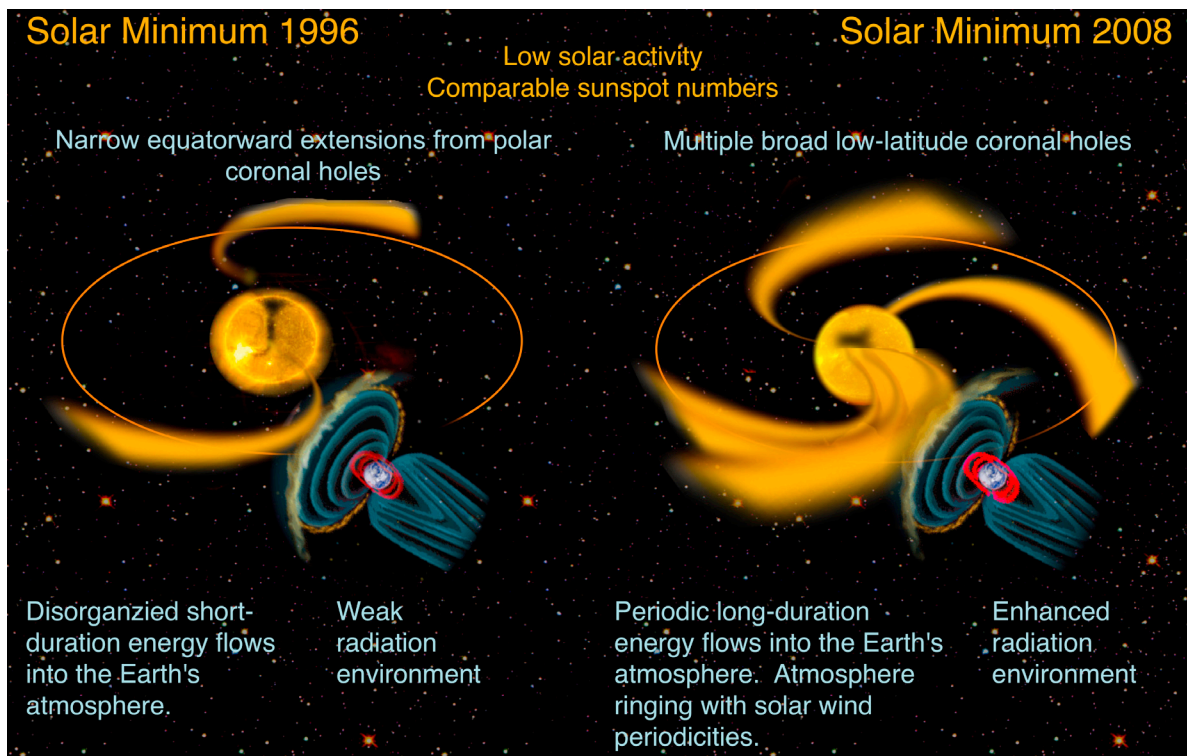


Figure 8. Artist's conception of origins and impacts of high-speed streams for two solar minima based on SoHO, *Wind* and GOES observations. The high-speed streams are indicated in yellow, the solar coronal holes that are the sources of the Earth-intersecting streams appear as dark regions on the central (yellow) images of the Sun. The Earth's magnetic fields are indicated in blue, and the radiation belts are indicated in red. [Gibson et al., 2009]

storms. Fast moving ICMEs drive interplanetary (IP) shocks in front of them, in effect forming a very large magnetosphere with a shock, magnetosheath and a magnetic bubble. These driven IP shocks are very efficient accelerators of energetic particles especially close to the Sun. But their impact at 1 AU is still not negligible. They can substantially enhance the already elevated radiation levels and compress the magnetosphere moving the radiation belts to lower altitudes. Despite decades of observation of these critical heliospheric structures, much is still unknown about them. Recent *Wind* observations, however, contributed to significant advances in this research area.

(1) *Remote observations of ICME driven IP shocks*

Low frequency Type II radio bursts (< 14 MHz) are produced by ICME-driven IP shocks and hence are excellent tools to remotely observe these shocks in a spatial domain outside the field-of-view of coronagraphs but not yet accessible to in-situ observations. The *Wind*/WAVES instrument, in collaboration with the similar STEREO instruments, provided some key observations in understanding the kinetics of the ICME/shock structure and the associated particle acceleration processes. *Gopalswamy et al.* [2008a] showed that coronal CME properties such as speed, width and solar-source longitude determine whether ICMEs will drive shocks and hence be associated with Type II radio bursts and SEP events. An interesting byproduct of this study was the determination that the Alfvén speed in the corona and in the near-Sun interplanetary medium can be anywhere from ~200 to ~1600 km/s, significantly different from the commonly assumed ~500 km/s value. This has important ramifications for the design of the *Solar Probe+* instruments. This factor of 4 variation in Alfvén speed explains why some fast ICMEs are radio quiet (RQ, i.e., without any Type II burst) and yet some slow ICMEs are radio loud (RL) [*Gopalswamy et al.*, 2008b]. A surprisingly large fraction (~34%) of IP shocks, observed in-situ at 1 AU, were radio quiet during their passage from the Sun [*Gopalswamy et al.*, 2010]. The solar CMEs associated with these RQ shocks were generally slow (average speed: ~535 km/s) while those associated with RL shocks were much faster (1237 km/s). Thus it emerges that the kinematics and particle acceleration efficiency of the ICME/shock structure is a complex function

of the variable ambient heliospheric magnetic field strength, CME speed, width and the relative orientation of the driven shock front and magnetic field direction.

(2) *CME speed profiles*

Measuring the speed of ICMEs is very difficult especially at altitudes above the range of coronagraphs. Recently, the WAVES Radio Experiment on *Wind* was used to derive precise speed profiles from the observed frequency drift of the decametric and kilometric Type II radio emissions for a large number of ICME-driven shocks as they propagated in interplanetary space [*Reiner et al.*, 2007]. It was found that ICME-driven shocks tend to decelerate rapidly near the Sun – the faster shocks decelerating more rapidly, but for shorter periods of time. For an event observed on April 4, 2000, it was determined that the resulting SEP acceleration occurred only during the first 6 hours after CME launch, i.e., only during the deceleration phase of the ICME/shock structure (see Figure 9). This result is consistent with the findings of *Gopalswamy et al.* [2009] that moderate speed CMEs stop driving shocks altogether, and therefore accelerating particles, by the time they reach a 3-4 Rs altitude, where the Alfvén speed peaks. Thus, the rapid deceleration of ICME-driven shocks near the Sun, where they are still fast moving, provides a natural explanation for the fact that SEP acceleration occurs preferentially only very close to the Sun.

(3) *The physical mechanism of the Type II radio bursts*

As described above, Type II radio burst observations have been successfully used to track ICME-driven shocks in the inner heliosphere. However, the physical mechanism by which a shock accelerates electrons and in turn converts this energy into radio bursts is not well understood. *Wind* remains the only mission that has published in-situ observations of a verified Type II source region. In a paper reporting the initial observations, *Bale et al.* [1999] showed that Type II radio bursts are generated in foreshock ‘bays’ upstream of IP shocks. For typical IP shocks, these foreshock ‘bays’ last only 10-15 seconds, thus they can be observed only by the very high time resolution *Wind* solar wind instruments. Recently, *Pulupa and Bale* [2008] used *Wind* measurements of velocity-dispersed electron beams at three IP shocks to measure the

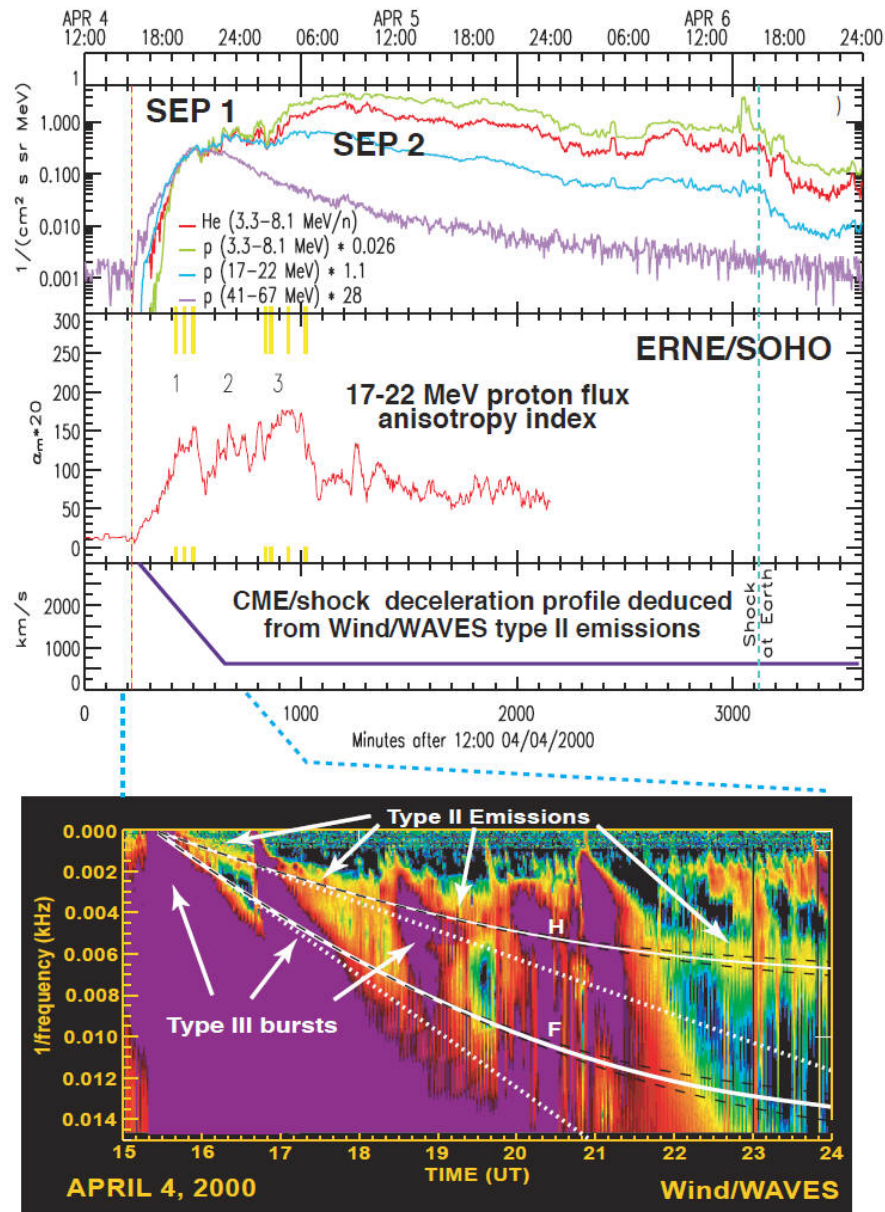


Figure 9. SEP fluxes and anisotropies for the 2000 April 4-6 ICME measured by the ERNE instrument on SoHO. The ICME/shock deceleration profile (lower panel) was deduced from the frequency drift of the Type II radio emissions observed by the WAVES experiment on *Wind*. [Kocharov *et al.*, 2009]

dimensions of these foreshock regions, finding that they are similar in size to the terrestrial bow shock. *Pulupa et al.* [2010] continued the investigation to determine statistically which shock and plasma parameters are correlated with upstream Langmuir wave activity. The analysis broadly confirmed the Fast Fermi picture of electron acceleration at shocks. However, some surprising results were also obtained, including the lack of any dependence on Mach number, and the greater importance on the

magnitudes of the up and downstream magnetic fields over the mirror ratio between the two values. This illustrates that continued study of this process is still necessary.

(4) Tracking ICMEs to 1 AU with white light images

While Type II radio bursts are very effective tools to follow the inner heliospheric motion of ICME-driven shocks, they cannot track the ICME material itself. STEREO Heliospheric Imager (HI)

observations can be used to identify at least the bright leading edges of ICMEs often all the way to 1 AU. However, line-of-sight effects make it difficult to reconstruct the true motion and size of the ICMEs. Recently, *Liu et al.* [2010] developed a triangulation technique that makes use of HI observations from both STEREO spacecraft and is able to accurately predict the arrival times and speeds of ICMEs at Earth. *Wind* observations were used to validate the method (see Figure 10). The method reveals non-radial motions and velocity changes of the ICME while traveling in the inner heliosphere. It also positively identifies the dark cavities in CME images with the magnetic flux rope structures observed in-situ. Thus *Wind* in-situ measurements together with STEREO white light observations resulted in a significantly better understanding of the kinetics of ICMEs.

(5) *Two-spacecraft reconstruction of the internal structure of magnetic clouds*

Considerable effort has been exerted to determine the internal structure of flux rope ICMEs, also known as magnetic clouds (MCs), at 1 AU. The Grad-Shafranov reconstruction technique enjoyed considerable success as this method does not assume a particular geometry (like cylindrical or elliptical cross-sections), but attempts to map the 1 AU cross section of a MC based on spacecraft observations constrained only by the MHD equations. Without the constraint of a specific geometry and based on only a single spacecraft track, however, there is a considerable level of uncertainty in the reconstruction. *Mostl et al.* [2008] were able to combine *Wind* and ACE observations of the same MC to improve the reliability of this method. Relying on their new results for the November 20, 2003 large ICME with SoHO and TRACE solar observations, they were able to estimate that ~50% of the MC's poloidal magnetic flux was lost through reconnection in interplanetary space. Merging *Wind* and STEREO observations of the May 23, 2007 MC, *Mostl et al.* [2009] and *Kilpua et al.* [2009] further refined their Grad-Shafranov techniques and found that for this cloud the internal field geometry turned out to be inconsistent with a classic force-free flux rope model. Moreover, the part of the MC closer to the Sun is non-force-free and is interacting with a trailing high speed stream. This result is consistent with the finding of *Kahler et al.* [2010] who used *Wind* energetic electron dispersion measurements of

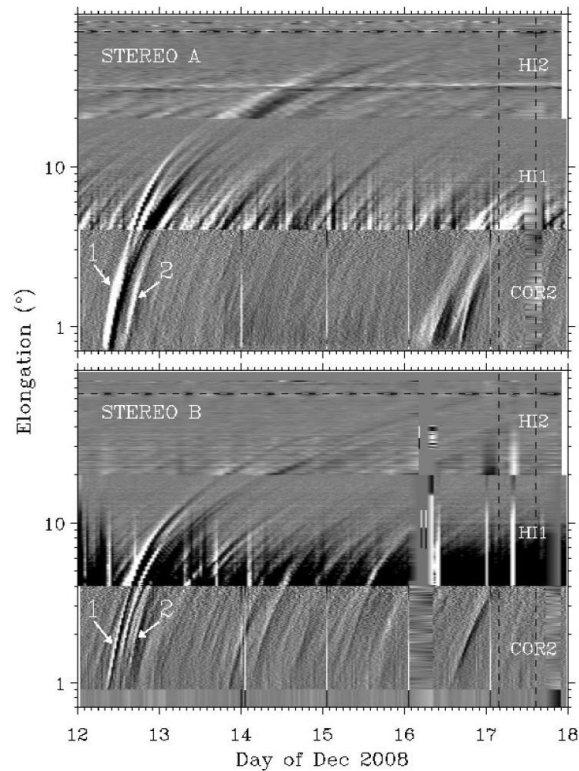


Figure 10. Time-elongation maps constructed from running difference images of COR2, HI1 and HI2 along the ecliptic plane for STEREO A (top) and B (bottom). The arrows indicate two tracks associated with the December 12, 2008 CME. The vertical dashed lines show the magnetic cloud time interval observed by *Wind* near Earth (horizontal dashed lines).

Type III radio burst related events inside magnetic clouds to determine the field line lengths traveled by the particles. The resulting travel distances were consistently shorter than what force-free flux rope models predicted. Thus, these new *Wind* results demonstrate that we still have a glaring lack of understanding of even the 1 AU internal structure of MCs.

(6) *Three-spacecraft reconstruction of the internal structure of a magnetic cloud*

The early phase of the STEREO mission afforded an unprecedented opportunity to observe near-Earth ICMEs with three spacecraft. Collecting *Wind* and STEREO B magnetic field and solar wind plasma measurements of the May 22, 2007 MC together, a combined magnetic field map was constructed by integrating the Grad-Shafranov equations [*Mostl et al.*, 2009]. Constraining the size of the cloud by the STEREO A observations, robust solutions for the

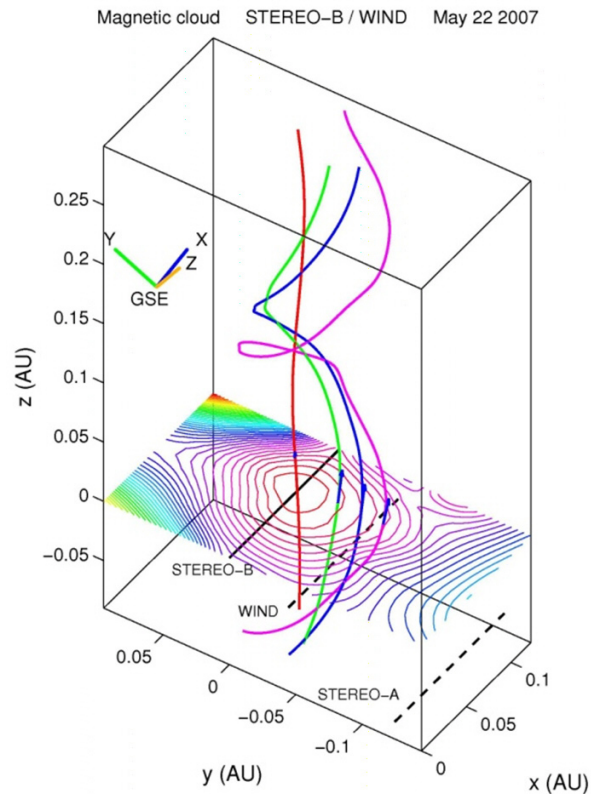


Figure 11. A 3D visualization of the magnetic cloud model generated using *Wind* and STEREO in-situ observations under the assumptions of translational invariance and time independence. The flux rope axis is inclined by about 60° to the ecliptic. This is the first three-spacecraft reconstruction of a magnetic cloud cross section. [Mostl *et al.*, 2009]

cross-sectional shape, for the orientation of the flux rope, and for the magnetic fluxes of the cloud were obtained. The results confirm the flux rope internal magnetic topology of MCs (even if they are not truly force-free), a basic assumption of most current MC models. The shape of the MC cross section was only slightly “flattened” or elliptical, with an aspect ratio of $\sim 1.5:1$ (see Figure 11). This is in contrast to the prediction of global MHD models whereby cloud cross sections are expected to significantly “flatten” or be elongated due to differential flows. This result provides new information that will be incorporated into global heliospheric models.

Future Plans:

During the prime phase of the STEREO mission the Sun was unusually quiet, launching only a handful of CMEs toward Earth, and thus limiting the originally envisioned two-spacecraft studies.

As the new solar cycle rises and the number of CMEs significantly increases, *Wind* observations with either STEREO spacecraft will be crucial as the two STEREO spacecraft will be too far apart to observe in-situ the same transients. Since *Wind* carries almost identical in-situ instruments to those on STEREO, multi-spacecraft studies of ICMEs will still be possible. In particular, past MC research focused on the cross-sectional shape of the flux ropes, but during the rising phase of the solar cycle the emphasis will be on the major radius curvature and global geometry of clouds. Also the internal magnetic topology and connectivity will be investigated with the aim to develop the next generation of MC models that include the expansion of clouds and their interaction with the ambient solar wind. In addition, the study of solar radio emission mechanisms, directivity and propagation in the inner heliosphere, using *Wind* and STEREO radio data will continue to pave the way for the upcoming *Solar Orbiter* and *Solar Probe+* missions.

2.3 HELIOPHYSICS OBJECTIVE #3: Geomagnetic Impact

The third and final heliophysics research objective of the *Science Plan for NASA’s Science Mission Directorate 2007-2016* concerns safeguarding the journey of exploration. To maximize the safety and productivity of human and robotic explorers, we must establish the geomagnetic impact of solar activity (as manifested in the 1 AU solar wind) to the point that the development of accurate forecasting capabilities becomes a possibility. *Wind* served as an upstream solar wind monitor or as the primary observation post (during its magnetotail crossing phase) for the studies summarized next. This objective also benefits from the ICME and shock studies described in the previous section.

2.3.1 Solar wind disturbances impacting the Earth’s magnetosphere

(1) Solar wind pressure pulse traveling through the magnetosheath

High speed solar wind streams and discontinuities compress the Earth’s magnetosphere resulting in harmful space weather events, like geomagnetic storms. However, before impacting the magnetopause, the solar wind disturbances have to travel through the bow shock and magnetosheath signifi-

cantly altering their character and making it difficult to accurately forecast their arrival times. *Maynard et al.*, [2008] studied an April 29, 2003 large tangential discontinuity that was observed in the upstream solar wind by *Wind* and in the magnetosheath by *Cluster*. The interaction of the tangential discontinuity and the accompanying pressure increase with the bow shock launched a fast wave and a slow mode structure in addition to the transmitted discontinuity itself. The fast wave traveling ahead of the discontinuity carried a significant portion of the pressure change, thus its arrival at the magnetopause was the crucial event determining the timing of the initial response of the magnetosphere. The fast wave was shown to be a planar structure, traveling at the magnetosonic speed nearly perpendicular to the magnetic field. Further case studies like this will be needed to develop a reliable space weather forecasting scheme.

(2) *The effect of the passage of a magnetic cloud on the magnetotail*

Magnetic clouds are the most geo-effective solar wind structures impacting the Earth's magnetosphere. The 2003 *Wind* passage of the deep magnetotail ($\sim -200 R_E$) serendipitously coincided with the passage of the November 20, 2003 magnetic cloud, that was also observed by ACE at the L1 point. *Wind*, nominally in the magnetosheath, observed a large expansion, twisting and tilting of the magnetotail as a result of the fivefold pressure drop at the front boundary of this magnetic cloud [*Farrugia et al.*, 2009]. These extreme conditions were in part responsible for *Wind* crossing the neutral sheet that was tilted by $\sim 85^\circ$ to the ecliptic, a highly unusual condition.

Future Plans:

Though *Wind* now is permanently stationed at L1, its historic deep magnetotail and numerous magnetospheric observations continue to be a fertile resource for the investigation of the geomagnetic impact of various solar wind structures. In particular, the unusual response of the Earth's magnetotail to the passage of the November 20, 2003 magnetic cloud will continue to be investigated with the aid of magnetospheric MHD models. Moreover, *Wind* will serve as the upstream solar wind monitor for future geo-effective solar wind events, the number of which is expected to significantly rise with the slowly increasing solar activity.

2.3.2 Forecasting the geomagnetic impact of magnetic clouds

The most geo-effective portion of very large magnetic clouds (it can take over a day for one to pass over the Earth's magnetosphere) is their prolonged and strong southward magnetic field sections. Based on a very large number of magnetic clouds observed by *Wind*, *Lepping et al.* [2009] has developed a scheme to automatically identify North-to-South type MCs in real-time, in order to forecast their typically associated magnetic storms. The scheme predicts the characteristics of the latter part of the N-to-S cloud based on measurements of its first 2/3 thus providing several hours of warning time. This program is expected to be applied to ACE real-time beacon data.

Future Plans:

A significant difficulty in accurately predicting the timing of geomagnetic activity due to an arriving ICME is that often not only the flux rope itself, but the driven sheath region in front of it is the cause of the activity. While there is much observational data and theoretical analysis regarding the standoff distance of Earth's bow shock, little is known about how this standoff distance (the thickness of the driven sheath region) for ICMEs varies from one ICME to another and how it varies as a function of heliocentric distance. To determine this standoff distance, the *Wind* and STEREO radio measurements will be combined with STEREO HI observations. Using the Type II radio bursts emanating from the driven shocks and the dark CME cavities in the HI images that are the flux ropes, careful analysis of the data sets will reveal the heliocentric variation of the standoff distance and will result in improved forecasting accuracy.

3. WIND SUPPORT FOR OTHER MISSIONS

As part of the Heliospheric Great Observatory, *Wind* has been contributing to numerous science investigations that rely on multi-spacecraft observations. Many of these have been described in the preceding sections. In addition, *Wind* observations are also critical to many other spacecraft, enabling and enhancing their mission success. In this section we outline some of these functions *Wind* serves.

3.1 Wind and STEREO

Because *Wind* carries the WAVES and the high time resolution 3DP solar wind experiments, it is the only near-Earth spacecraft that can serve as backup for the STEREO in-situ and radio observations. Together with SOHO, *Wind* can recover all of the scientific objectives of the STEREO mission should one of the twin spacecraft become incapacitated.

Even assuming a long and healthy life for STEREO, the two spacecraft, separating from each other at 44 degrees/year, are already too far separated in longitude for ideal stereoscopic observations. During 2010-2011, the two STEREO spacecraft will be on opposite sides of the Sun. Clearly by this time, and long before it, the heliospheric imager of one cannot see the solar wind structures that flow past the other. However, *Wind*, being half way between them, will be ideally positioned to carry out the in-situ observations for both spacecraft. Thus *Wind* is crucial for the success of a STEREO extended mission, especially with the already increasing solar activity.

During 2012-2013, the two STEREO spacecraft and *Wind* will be nearly equally displaced from each other at $\sim 120^\circ$. This configuration will be ideal for global heliospheric studies and for the testing of global heliospheric models. The two STEREO spacecraft and SDO will image the complete solar surface providing inner boundary conditions for global MHD models. Then *Wind*, along with the two STEREO spacecraft, will measure the 1 AU in-situ solar wind conditions to validate model predictions at widely displaced positions. ***Thus, Wind is in essence the third in-situ "eye" of the STEREO mission.***

3.2 Wind and ACE

Wind and ACE have been mutually supporting each other in refining the calibrations of their instrumentation. Since *Wind* determines and intercalibrates its solar wind plasma measurements from three different instruments that operate based on different physical principles (SWE, 3DP and WAVES), it supplies highly accurate and independent estimates of thermal plasma key parameters. In addition, the SWE instrument can operate through the high-energy particle showers associated with flares and CMEs. Thus the *Wind* data is very robust. The ACE SWEPAM team takes full advantage of these

Wind solar wind plasma observations to improve their calibrations. This cooperation is expected to continue through the upcoming years.

Magnetic field measurement also mutually benefit from intercalibrations between *Wind* and ACE. On spinning spacecraft, the highest accuracies are achieved for the spacecraft spin plane components. Since the *Wind* and ACE spin axes are perpendicular, the lower quality, spin axis component calibrations can be improved by comparing them to the appropriate spin plane component from the other spacecraft whenever they are sufficiently close to each other.

Finally, while ACE dominates high energy particle observations, the *Wind*/EPACT/LEMT telescope fills in an important gap in the 1-10 MeV/nucleon range between the ULEIS and SIS instruments on ACE. Since *Wind* is an ecliptic north spinner, unlike ACE detectors, the LEMT instrument also collects anisotropy information of the energetic particle distributions and can detect backstreaming populations from outer heliospheric shocks [e.g., *Tan et al.*, 2009]. Moreover, because of its large collecting area, EPACT can also measure the scientifically interesting smaller prompt solar energetic particle events. In summary, ***Wind provides significant calibrational information to ACE, complements its measurements and facilitates collaborative, multi-spacecraft studies.***

3.3 Wind and RHESSI

RHESSI provides imaging and spectroscopy of the hard X-ray/gamma-ray continuum and gamma-ray lines emitted by energetic electrons and ions, respectively. RHESSI accurately locates these particles at the Sun, and its precise spectral measurements provide information on the spectra of the parent electrons and ions, and on the ion composition. *Wind*, using the 3DP and EPACT experiments, provides unique in-situ measurements of the energetic electrons and ions that reach ~ 1 AU, and, with WAVES, of the radio emissions produced by the energetic electrons while traveling from the Sun to 1 AU. In a 1995 study, *Kiplinger* [1995] found that flares with hard X-ray spectra that evolved from soft to hard to harder (SHH) are closely associated with SEP events observed in interplanetary space. In a statistical study of all RHESSI flares in combination with *Wind*/3DP observations, *Saldanha et al.* [2008] and *Grayson et al.* [2009] confirmed *Kiplinger's* work; all RHESSI flares associated with

an SEP event show SHH behavior and none of the flares with SHS behavior are associated with an SEP. While the physical association between the progressively hardening X-ray spectrum and the particles is not understood at present, the results strongly suggest a physical connection between the X-ray-producing electrons in the flare on closed flare loops and the escaping energetic protons on open field lines. This correlation is puzzling and will require further investigations, since it is generally believed that an interplanetary shock front, remote from the flare itself, is the main accelerator. *Wind* will continue to support this and similar RHESSI research projects.

3.4 Wind and IBEX, Voyagers, MESSENGER

Since the IMP 8 magnetometer stopped returning data in 2000, the *Wind* observations have usually supplied the 1 AU baseline for deep space observations such as those by the *Voyagers*, and more recently for MESSENGER. The robust and continuous *Wind* solar wind measurements are essential for studies ranging from the predicted position of the termination shock, observed remotely by IBEX, to the evolution of solar wind transients from the inner heliosphere. As MESSENGER will settle into a Mercury orbit and turn on its full instrumentation, studies of the inner heliospheric evolution of solar wind transients will be supported by the 1 AU *Wind* observations.

3.5 Wind and ARTHEMIS, Cluster

Two of the THEMIS spacecraft, called ARTHEMIS, are now in permanent lunar orbits spending a large fraction of their time in the ambient solar wind. *Wind*, together with the two ARTHEMIS spacecraft, will provide unprecedented multi-point plasma measurements at the uniquely high, 3 second cadence that will address the fundamental question of whether the reconnection X-lines for low magnetic shears are generally patchy or extended. Multi-point high-resolution measurements with *Cluster* and ARTHEMIS will also be used to investigate the structure of the reconnection exhaust as a function of the distance from the X-line.

3.6 Wind and RBSP, MMS

The launch of the two RBSP spacecraft is presently scheduled for May 2012, and of the MMS spacecraft for 2014, during the period covered by

this Senior Review. In its detailed description of the scientific objectives for the mission, the RBSP Science Working Group has identified a need for solar wind observations to determine the occurrence patterns of the various acceleration, transport, and loss processes for relativistic, near-relativistic, and ring current particles within the Earth's inner magnetosphere. *Wind* observations of the solar wind plasma and magnetic field will prove ideal for this purpose and for the similar science objectives of the MMS mission.

3.7 Wind and Swift, Fermi

Cosmic gamma ray bursts (GRBs) are transients of large red-shift, and take place at least 600 times per year from the entire visible universe. GRBs have time durations of seconds or more, with photon energies ranging from the hard X-ray to very high energy gamma-ray. Only 1 GRB is ever seen from any 1 source (since each is presumably a stellar birth/death signal).

Soft gamma repeaters (SGRs) are of somewhat less visible intensity, but with orders of magnitude less absolute magnitude, since their sources are in our Milky Way galaxy and its immediate neighbors, including the Magellanic Clouds. SGRs repeat at random, often or rarely, from a few times up to hundreds of times over spans from days to months. There are only half a dozen known SGR sources.

Giant Flares (GFs) are of greater apparent intensity than GRBs and are very rare, averaging once per decade. GFs are emitted from the source objects of the SGRs, one or none from each source, to date.

The KONUS instrument on *Wind* was designed to study GRBs, SGRs, and GFs, with omnidirectional sensitivity to all gamma-ray transients. Its scientific data fall roughly into the following categories: KONUS detects on the average the brightest 120 GRBs per year, thus providing comparison data for many of the Swift GRBs. In particular, KONUS provides the higher energy determination that is beyond *Swift*'s energy range. Secondly, KONUS is a key vertex in the Interplanetary GRB Network (IPN), composed of *Swift*, *Fermi*, *Mars Odyssey*, MESSENGER, INTEGRAL, AGILE, *Suzaku*, and HETE-2. The IPN finds the source directions of transients by virtue of its timing geometry, independently of oriented telescopes. KONUS is generally the most sensitive of these to SGRs, an advantage that result from its lack of collimation.

Due to the rarity of these astrophysical events, an additional four years of *Wind* KONUS observations will significantly enhance the events collected by *Swift*, *Fermi* and the IPN.

4. TECHNICAL AND BUDGET SECTION

4.1 Spacecraft Health

The *Wind* spacecraft continues in very good health. The communication system was successfully reconfigured in 2000 to realize an enhancement in telemetry margin. Reliance on a single digital tape recorder since the 1997 failure of the backup unit has never hampered operations, and measures were taken to minimize its use to extend its life. During the past few years, the spacecraft experienced a few instrument latch-ups and single bit flight software errors most likely due to high energy particle single event upsets. These events served to exercise the spacecraft and instrument recovery procedures and showed that within a couple of days, all instruments can be brought back to full science operations. Two of the three spacecraft batteries experienced periods of excess charging, causing battery #2 to heat up. A mode change was implemented to adjust the charge current and the temperature returned to nominal values. Battery #1 charge currents and temperatures are being closely monitored. There are several modes available with which to manage the battery situation. None of these events appear to have lasting impacts.

Wind continues to have a large fuel reserve. The latest analysis shows that 58 kg fuel remains, which is equivalent of approximately 114 m/sec of radial delta-V assuming normal thruster operations. To maintain its current orbit around the L1 point, *Wind* needs to carry out four station keeping maneuvers every year. These maneuvers are very similar and require about 0.5 m/sec delta-V each. Thus, barring any other cause, *Wind* has enough fuel to maintain its orbit for nearly 60 years.

4.2 Instrument Status

Seven of the eight *Wind* instruments, including all of the fields and particles suits, remain largely or fully functional. The only instrument turned off is the TGRS γ -ray instrument that was designed for only a few years of operations. The general status of all instruments is summarized in Table 2.

The specific degradations in instrument capabil-

ities are the following: The APE and IT detectors of the EPACT instrument, covering the highest energy ranges, do not work. But the LEMT and STEP telescopes of the same instrument continue to operate normally, providing crucial and unique observations of solar energetic particles up to 10 MeV in energy. On the SMS instrument the SWICS solar wind composition sensor had to be turned off in May 2000. The SMS DPU experienced a latch-up reset on 26 June 2009 that placed the MASS acceleration/deceleration power supply into a fixed voltage mode, rather than stepping through a set of voltages. It has been determined that a moderate risk power cycling of the SMS DPU would be required to fix this problem. In order to protect the unique and fully functional STICS sensor, it has been decided to leave the MASS sensor in a fixed voltage mode that allows reasonable but reduced science data collection. Finally, the VEIS thermal electron detectors on the SWE instrument experienced high voltage problems in November, 2001. This problem was resolved by reprogramming the SWE Strahl sensor to recover most of the original functions. Moreover, the 3DP instrument also covers the impacted electron measurements making these observations still redundant and hence robust. All of the other instruments continue to function fully.

4.3 Ground Operations

Wind ground operations takes place at Goddard and is currently transitioned from the legacy *Polar-Wind-Geotail* system to Multi-Mission Operations Center (MMOC) that consolidates *Wind* operations with that of ACE and TRACE. This transition became necessary with the decommissioning of *Polar* on April 30, 2008 and it includes the upgrade of outdated and costly to maintain hardware and software. The Operational Readiness Review of the MMOC is scheduled for March 31, 2010.

For cost saving measures, the flight operations team reduced staffing by 1 FTE in November 2008 and modified shift schedules to reduce operational coverage from twelve to eight hours (reducing the need for overtime and shift differential). With the successful transition of *Wind* flight operations into the MMOC, the staffing levels will be further adjusted to operate the ACE, *Wind* and TRACE missions with a combined team that also includes non-traditional flight operations skills (HW/SW maintenance, Flight Dynamics attitude analysis). Re-engineering/

Table 2. The status of the *Wind* instrument.

Instrument	Principal Investigator	Institution	Status
SWE	K. W. Ogilvie	Electrons: GSFC, UNH Ions: MIT	Strahl detector reconfigured Faraday Cup fully operational
3DP	R. P. Lin	UC Berkeley	Fully operational
MFI	A. Szabo	GSFC	Fully operational
SMS	S. Lepri	U. Michigan	SWICS turned off MASS reduced coverage STICS fully operational
EPACT	T. Von Rosenvinge	GSFC	APE, IT turned off LEMT, STEP operational
WAVES	R. MacDowall J.-L. Bougeret	GSFC Paris Observatory	Fully operational
KONUS	E. Mazets	Ioffe Institute, Russia	Fully operational
TGRS	B. Teegarden	GSFC	Turned off

upgrading existing systems will promote efficiency with respect to implementing IT Security and HW/SW maintenance as well as system administration. Automation is being implemented with a unified approach to further increase efficiency. The teams will continue to cross train at multiple positions so that prime and backup roles are covered. In spite of the disruptions due to the transitioning of operation to the MMOC, data recovery for *Wind* for the last two years averaged 98%. Most of the unrecoverable data loss occurred when *Wind* Deep Space Network supports were released for other spacecraft launches and emergencies with some data loss resulting also from network problems.

The current operation of *Wind* requires one ~2 hour DSN support per day. This allows the up-linking of the daily Stored Command Table load and the playback of the Digital Tape Recorder. *Wind* also maintains real-time solar wind monitoring during these 2 hour contacts. In 2001, an attempt was made to reduce the number of DSN contacts, and hence the cost of operations, by scheduling DSN time only once every three days, albeit for longer durations. Reducing the number of contacts saves the lengthy setup and reset times. After extensive testing it was concluded that this scenario did not provide significant savings and introduced critical risks to the mission. *Wind* can store only three days worth of commands, thus this is the longest *Wind* can go without ground contact or the spacecraft performs an emergency load shed. Hence the current

flexibility to negotiate contact time with DSN was eliminated. Also, all of these infrequent contacts had to be fully attended regardless of the time of day. Currently about half of the contacts are completely automated allowing the operation staff to keep day schedules. Thus, the current daily contact scenario is considered optimal.

The *Wind* mission operations team is currently investigating the possibility of leaving the *Wind* transmitter on at all times, thus providing 24/7 real-time capability. The tests are expected to be completed by the end of March, 2010.

The distribution and archiving of all level zero files and the production of the quick-look key parameter (KP) files also takes place at Goddard, but in the Science Directorate under the control of the project scientist. The two server (plus backup) system was re-engineered in 2006 and is not expected to require any significant upgrades during the next four years.

4.4 In-Guide Budget

The in-guide budget described in this section will fund the mission operations necessary to continue the safe operation of the *Wind* spacecraft along with basic data reduction and validation processes performed at the various instrument institutions. As in the previous years, the scientific research outlined in the previous sections are expected to be funded through the Guest Investigator program with each element individually proposed and peer reviewed.

4.4.1 Mission Operations

The inputs in the budget spreadsheet Table II are the direct costs to the *Wind* project. Line 2b is Mission Services and includes the flight operations team at a contractor WYE level of 4.0 in FY10, with a reduction to 3.5 planned in FY11 through FY14, as a result of the ground system re-engineering effort of the MMOC. Also included in Line 2b is support from flight dynamics for orbit determination and station keeping maneuvers at a contractor WYE level of 0.5. Line 2b also includes the DSN scheduling work at a contractor WYE level of 0.5. The sustaining engineering cost for FY10-14 is for system administration of the MMOC. Line 2c represents the civil servant salary for a Mission Director, which is charged at .3 FTE.

Table IV provides the “In Kind” costs. These are services provide to *Wind* that are funded by other sources. These costs are allocated to *Wind*, but are not supported with Project funds. Line 2a includes the use of the Deep Space Network apertures as well as the cost of voice and data connections at GSFC. Line 2b includes some transition support for the reengineering effort in FY10, and an allocation of costs for Uninterruptible Power Systems and building engineers in the Mission Operations Building at GSFC. Line 2c represents costs allocated by the SSMO Project for all the elements associated with Project Management and for use of the Mission Operations and Mission Services (MOMS) contract.

Maintaining the *Wind* portion of the reengineered PWG system will require the support of a software engineer at the 0.3 FTE level. The PWG system is responsible for the archival of the level zero data and its distribution to the instrument sites and for the generation of the quick-look key parameter (KP) data files. Therefore, the associated costs are listed on line 3 as Science Operations Functions. Since the PWG system hardware has been refreshed during the past two years, our expectation is that an initial modest \$2.0K/year level, ramping up to \$10K/year by FY13, would be sufficient to maintain the system. In addition, a \$1.1K/year ODIN fee has to be paid to maintain active software licenses. These costs are listed under project management in Table III, since it operates under direct Code 600 supervision. The overall Goddard project management costs have been significantly reduced and besides the PWG system, it includes only 0.2-0.3 FTE of

time shared between the project scientist and deputy project scientist and 0.2 FTE for a contract resource analyst. Even with this reduction, almost 50% of the in-guide funding is needed for mission operations (40%) and project management (7%).

4.4.2 Science Data Production

The other half of the requested in-guide funding is allocated to the generation, calibration and validation of the various *Wind* instrument data products. After receiving the level zero instrument data along with housekeeping and ephemeris information, the instrument teams are responsible for the generation of science quality data that is fully calibrated and validated typically through the performance of well established scientific analysis. In addition, they have to provide full, data granule level description and intermediate-term archiving (i.e., guaranteed backups till final submission to SPDF/CDAWeb or NSSDC). In addition, the occasional *Wind* maneuvers (about 4/year for station keeping) necessitate instrument level commanding that the instrument teams are required to support. Thus, besides data production expertise, the teams have to maintain a low level engineering capability that can support routine and emergency operations. Finally, since *Wind* does not have a project level science center, the instrument teams are responsible for the public dissemination of their data through the maintaining of Web pages.

Due to the limited funding available, the instrument teams optimized their operation to stay roughly within 1 FTE for all aspects of operation. All fully functional instruments (MFI, SWE/Electron, SWE/Faraday Cup, WAVES, 3DP) are allocated almost exactly the same amount of support, regardless whether they are full cost accounted Goddard civil service or university operations. It should be noted that SWE is composed of two independent instruments: the Goddard electron instrument and the MIT Faraday Cup. They each have the same allocation, but are reported together.

The two partially functioning instruments (EPACT and SMS) are allocated about half as much as their data production requirements are significantly diminished. However, they still continue to produce valuable data, therefore their continued support at this reduced level is still requested. The astrophysical KONUS instrument received in the past a minimal amount of funding (\$20K/year) mostly to support project level documentation. This instrument

receives some minor amount of funding in Russia for data production and even less support from the *Swift* mission for a part time Goddard contractor. Thus no new funding is requested for them in this proposal.

The final budget elements is education and public outreach that is combined for all instruments and is at the ~1% level of the project total. As it is described in the E/PO section, this funding is proposed to be combined with that of the STEREO project for a more substantial effort.

REFERENCES

- Bale, S. D., M. J. Reiner, J.-L. Bougeret, M. L. Kaiser, S. Krucker, D. E. Larson and R. P. Lin, (1999), The source region of an interplanetary Type II radio burst, *Geophys. Res. Lett.*, *26*, 1573-1576, doi:10.1029/1999GL900293.
- Bale, S. D., What keeps the solar wind hot? (2008), *Physics*, *1*, 42.
- Brown, J. C., R. Turkmani, E.P. Kontar, A.L. MacKinnon and L. Vlahos, Local re-acceleration and a modified thick target model of solar flare electrons (2009), *Astron. Astrophys.*, *508*, 2, 993-1000.
- Cranmer, S. R., G. B. Field and J. L. Kohl, (1999), Spectroscopic constraints on models of ion cyclotron resonance heating in the polar solar corona and high-speed solar wind, *Astrophys. J.*, *518*, 937.
- Edmiston, J. P. and C. F. Kennel, A parametric survey of the first critical Mach number for a fast MHD shock (1984), *J. Plasma Phys.*, *32*, 429-441.
- Endeve, E., O. Lie-Svendsen, V. H. Hansteen and E. Leer, (2005), Release of helium from closed-field regions of the Sun, *Astrophys. J.*, *624*, 402-413, doi:10.1086/381239.
- Eriksson, S., J. T. Gosling, T. D. Phan, L. M. Blush, K. D. C. Simunac, D. Krauss-Varban, A. Szabo, J. G. Luhmann, C. T. Russell, A. B. Galvin, and M. H. Acuna, (2009), Asymmetric Shear-Flow Effects on Magnetic Field Configuration Within Oppositely Directed Solar Wind Reconnection Exhausts, *J. Geophys. Res.*, *114*, A07103, doi:10.1029/2008JA013990.
- Eviatar, A. and M. Schultz (1970), Ion-temperature anisotropies and structure of solar wind, *Planet. Space Sci.*, *18*, 321.
- Farrugia, C. J., E. V. Erkaev, N. C. Maynard, I. G. Richardson, P. E. Sandholt, D. Langmayr, K. W. Ogilvie, A. Szabo, U. Taubenschuss, R. B. Torbert and H. K. Biernat (2009), Effects on the distant geomagnetic tail of a fivefold density drop in the inner sheath region of a magnetic cloud: A joint Wind-ACE study, *Adv. Space Res.*, *44*(11) 1288.
- Gary, S. P. (1981), Microinstabilities upstream of the Earth's bow shock – A brief review, *J. Geophys. Res.*, *86*, 4331-4336, doi:10.1029/JA086iA06p04331.
- Gary, S. P., E. E. Scime, J. L. Phillips and W. C. Feldman (1994), The whistler heat flux instability: Threshold conditions in the solar wind, *J. Geophys. Res.*, *99*, 23,391, doi:10.1029/94JA02067.
- Gary, S. P., R. M. Skoug and W. Daughton (1999), Electron heat flux constraints in the solar wind, *Phys. Plasmas*, *6*, 2607-2612, doi:10.1063/1.873532.
- Gibson, S. E., J. U. Kozyra, G. de Toma, B. A. Emery, T. Onsager and B. J. Thompson (2009), If the Sun is so quiet, why is the Earth ringing? A comparison of two solar minimum intervals, *J. Geophys. Res.*, *114*, A09105, doi:10.1029/2009JA014342.
- Goldstein, B., M. Neugebauer, L. D. Zhang and S. P. Gary (2000), Observed constraints on proton-proton relative velocities in the solar wind, *Geophys. Res. Lett.*, *27*, 53-56.
- Gopalswamy, N., S. Yashiro, H. Xie, S. Akiyama, E. Aguilar-Rodriguez, M. Kaiser, R. A. Howard and J.-L. Bougeret (2008a), Radio-quiet fast and wide coronal mass ejections, *Astrophys. J.*, *674*, 560.
- Gopalswamy, N., S. Yashiro, S. Akiyama, P. Makela, H. Xie, M. Kaiser, R. A. Howard and J.-L. Bougeret (2008b), Coronal mass ejections, Type II radio bursts, and solar energetic particle events in the SOHO era, *Ann. Geophys.*, *26*(10), 3033-3047.
- Gopalswamy, N., W. T. Thompson, J. M. Davila, M. L. Kaiser, S. Yashiro, P. Makela, G. Michalek, J.-L. Bougeret and R. A. Howard (2009), Relation between Type II bursts and CEMs inferred from STEREO observations, *Sol. Phys.*, *259*, 227.
- Gopalswamy, N., H. Xie, P. Makela, S. Akiyama, S. Yashiro, M. Kaiser, R. A. Howard and J.-L. Bougeret (2010), Interplanetary shocks lacking Type II radio bursts, *Astrophys. J.*, *710*, 1111.
- Gosling, J. T., R. M. Skoug, D. J. McComas, and C. W. Smith (2005), Direct Evidence for Magnetic Reconnection in the Solar Wind near 1 AU, *J. Geophys. Res.*, *110*, A01107, doi:10.1029/2004JA010809.
- Gosling, J. T., S. Eriksson, T. D. Phan, D. E. Larson, R. M. Skoug, and D. J. McComas (2007a), Direct Evidence for Prolonged Magnetic Reconnection at a Continuous X-Line Within the Heliospheric Current Sheet, *Geophys. Res. Lett.*, *34*, L06102, doi:10.1029/2006GL029033.
- Gosling, J. T., S. Eriksson, L. Blush, T. D. Phan, J. G. Luhmann, D. J. McComas, R. M. Skoug, M. H. Acuna, C. T. Russell, and K. D. Simunac (2007b), Five Spacecraft Observations of Oppositely Directed Exhaust Jets from a Magnetic Reconnection X-line Extending $> 4.26 \times 10^6$ km in the Solar Wind at 1 AU, *Geophys. Res. Lett.*, *34*, L20108, doi:10.1029/2007GL031492.
- Gosling, J. T., T. D. Phan, R. P. Lin, and A. Szabo (2007c),

- Prevalence of Magnetic Reconnection at Small Field Shear Angles in the Solar Wind, *Geophys. Res. Lett.*, *34*, L15110, doi:10.1029/2007GL030706.
- Gosling, J. T., and A. Szabo (2008), Bifurcated Current Sheets Produced by Magnetic Reconnection in the Solar Wind, *J. Geophys. Res.*, *113*, A10103, doi:10.1029/2008JA013473.
- Grayson, J. A., S. Krucker and R. P. Lin (2009), A statistical study of spectral hardening in solar flares and related solar energetic particle events, *Astrophys. J.*, *707*, 1588.
- Hernandez, R., S. Livi and E. Marsch (1987), On the He²⁺ to H⁺ temperature ratio in slow solar wind, *J. Geophys. Res.*, *92*, 7723.
- Kahler, S., S. Krucker and A. Szabo (2010), Solar energetic electron probes of magnetic cloud field-line lengths, *J. Geophys. Res.*, submitted, doi:10.1029/2010JA015328.
- Kasper, J. C., A. J. Lazarus, J. T. Steinberg, K. W. Ogilvie and A. Szabo (2006), Physics-based tests to identify the accuracy of solar wind ion measurements: A case study with the Wind Faraday Cups, *J. Geophys. Res.*, *111*, A03105.
- Kasper, J. C., M. L. Stevens, A. J. Lazarus, J. T. Steinberg and K. W. Ogilvie (2007), Solar wind helium abundance as a function of speed and heliographic latitude: Variation through a solar cycle, *Astrophys. J.*, *660*, 901.
- Kasper, J. C., A. J. Lazarus and S. P. Gary (2008), Hot Solar-Wind Helium: Direct Evidence for Local Heating by Alfvén-Cyclotron Dissipation, *Phys. Rev. Lett.*, *101*, 261103.
- Kennel, C. F., Critical Mach numbers in classical magnetohydrodynamics (1987), *J. Geophys. Res.*, *92*, 13,427-13,437, doi:10.1029iA12p13427.
- Kepko, L. and H. E. Spence (2003), Observations of discrete, global magnetospheric oscillations directly driven by solar wind density variations, *J. Geophys. Res.*, *108*, A6, 1257, doi:10.1029/2002JA009676.
- Kepko, L., J. E. Spence and H. J. Singer (2002), ULF waves in the solar wind as direct drivers of magnetospheric pulsations, *Geophys. Res. Lett.*, *39*(8), 1197, doi:10.1029/2001GL014405.
- Kilpua, E. K. J., P. C. Liewer, C. J. Farrugia, J. G. Luhmann, C. Mostl, Y. Li, Y. Liu, B. J. Lynch, C. T. Russell, A. Vourlidas, M. H. Acuna, A. B. Galvin, D. E. Larson and J. A. Sauvaud (2009), Multispacecraft observations of magnetic clouds and their solar origins between 19 and 23 May 2007, *Solar Phys.*, *254*, 325-344.
- Kiplinger, A. L. (1995), Comparative studies of hard X-ray spectral evolution in solar flares with high energy proton events observed at Earth, *Astrophys. J.*, *453*, 973.
- Ko, Y. K., A. J. Tylka, C. K. Ng and Y.-M. Wang (2010), Solar wind source regions and variability on heavy-ion composition in gradual solar energetic particle events, *Astrophys. J. Lett.*, Submitted.
- Kocharov, L., T. Laitinen, A. Al-Sawad, O. Saloniemi, E. Valtonen and M. J. Reiner (2009), Gradual solar energetic particle event associated with a decelerating shock wave, *Astrophys. J. Lett.*, *700*(1), L51-L55.
- Krucker, S., E. P. Kontar, S. Christe and R. P. Lin (2007), Solar flare electron spectra at the Sun and near the Earth, *Astrophys. J.*, *663*, L109-L112.
- Lavraud, B., J. T. Gosling, A. P. Rouillard, A. Fedorov, A. Opitz, J.-A. Sauvaud, C. Foullon, I. Dandouras, V. Genot, C. Jacquy, P. Louarn, C. Mazelle, E. Penou, T. D. Phan, D. E. Larson, J. G. Luhmann, P. Schroeder, R. M. Skoug, J. T. Steinberg and C. T. Russell (2009), Observations of a Complex Solar Wind Reconnection Exhaust from Spacecraft Separated by over 1800 R_E, *Solar Physics*, *256*, 379-392, doi:10.1007/s11207-009-9341-x.
- Leitner, M., C. J. Farrugia, A. B. Galvin, H. K. Biernat and V. A. Osherovich (2009), The solar wind quasi-invariant observed by STEREO A and B at solar minimum 2007, and comparison with two other minima, *Solar Phys.*, *259*, 381-388.
- Leitner, M., C. J. Farrugia and Z. Voros (2010), Change of solar wind quasi-invariant in solar cycle 23 – Analysis of PDFs, *J. Atmos. Solar-Terr. Phys.*, in press.
- Lepping, R. P., T. W. Narock and C.-C. Wu (2009), A scheme for finding the front boundary of an interplanetary magnetic cloud, *Ann. Geophys.*, *27*, 1-17.
- Liu, Y., J. A. Davis, J. G. Luhmann, A. Vourlidas, S. D. Bale and R. P. Lin (2010), Geometric triangulation of imaging observations to track coronal mass ejections continuously out to 1 AU, *Astrophys. J. Lett.*, *710*, L82-L87, doi:10.1088/2041-8205/710/1/L82.
- Luhmann, J. G., C. O. Lee, Y. Li, C. N. Arge, A. B. Galvin, K. Simunac, C. T. Russell, R. A. Howard and G. Petrie (2009), Solar wind sources in the late declining phase of Cycle 23: Effects of the weak solar polar field on high speed streams, *Solar Phys.*, *256*, 285-305.
- Mason, G. M. (2007), ³He-rich solar energetic particle events, *Space Sci. Rev.*, *130*, 131-142.
- Marsch, E., C. K. Goertz and K. Richter (1982), Wave heating and acceleration of solar wind ions by cyclotron resonance, *J. Geophys. Res.*, *87*, 5030-5044.
- Marsch, E. (2006), Kinetic physics of the Solar corona and solar wind, *Living Rev. Solar Phys.*, *3*.
- Maynard, N. C., C. J. Farrugia, D. M. Ober, W. J. Burke, F. S. Mozer, H. Reme, P. Decreau and K. D. Siebert (2008), Cluster observations of fast waves in the magnetosheath launched as a tangential discontinuity with a pressure increase crossed the bow shock, *J. Geophys. Res.*, doi:10.1029/2008JA013121.

- Mellott, M. M., and E. W. Greenstadt (1984), The structure of oblique subcritical bow shock – ISEE 1 and 2 observations, *J. Geophys. Res.*, *89*, 2151-2161, doi:10.1029/JA089iA04p02151.
- Mostl, C., C. Miklenic, C. J. Farrugia, A. Veronig, M. Temmer, A. B. Galvin, B. Vrsnak and H. K. Biernat (2008), Two-spacecraft reconstruction of a magnetic cloud and comparison to its solar source, *Ann. Geophys.*, *26*, 3139-3152.
- Mostl, C., C. J. Farrugia, H. K. Biernat, A. B. Galvin, J. G. Luhmann and E. K. J. Kilpua (2009), Optimized Grad-Shafranov reconstruction of a magnetic cloud using STEREO-Wind observations, *Solar Phys.*, *256*, 427-441.
- Osherovich, V. A., J. Fainberg and R. G. Stone (1999), Solar wind quasi-invariant as a new index of solar activity, *Geophys. Res. Lett.*, *26*, 16, 2597-2600, doi:10.1029/1999GL900583.
- Petkaki, P., M. P. Freeman, T. Kirk, C. E. J. Watt and R. B. Horn (2006), Anomalous resistivity and the nonlinear evolution of the ion-acoustic instability, *J. Geophys. Res.*, *111*, 1205, doi:10.1029/2004JA010793.
- Phan, T. D., J. T. Gosling, M. S. Davis, R. M. Skoug, M. Oieroset, R. P. Lin, R. P. Lepping, D. J. McComas, C. W. Smith, H. Reme and A. Balogh (2006), A Magnetic Reconnection X-line Extending more than 390 Earth Radii in the Solar Wind, *Nature*, *439*, 175-178.
- Phan, T. D., J. T. Gosling, and M. S. Davis (2009), Prevalence of Extended Reconnection X-lines in the Solar Wind at 1 AU, *Geophys. Res. Lett.*, *36*, L09108, doi:10.1029/2009GL037713.
- Pulupa, M. and S. D. Bale (2008), Structure on interplanetary shock fronts: Type II radio burst source regions, *Astrophys. J.*, *676*, 1330-1337, doi:10.1086/526405.
- Pulupa, M. S. D. Bale and J. C. Kasper (2010), Langmuir waves upstream of interplanetary shocks: Dependence on shock and plasma parameters, *J. Geophys. Res.*, in press.
- Reames, D. V. (2009), Solar energetic particle release times in historic ground level events, *Astrophys. J.*, *706*, 844-850.
- Reiner, M. J., M. L. Kaiser, J.-L. Bougeret (2007), Coronal and interplanetary propagation of CME/shocks from radio, in situ and white light observations, *Astrophys. J.*, *663*(2), 1369-1385.
- Saito, S. and S. P. Gary (2007), Whistler scattering of suprathermal electrons in the solar wind: Particle-in-cell simulations, *J. Geophys. Res.*, *112*, 6116, doi:10.1029/2006JA012216.
- Saldanha, R., S. Krucker and R. P. Lin (2008), Hard X-ray spectral evolution and production of solar energetic particle events during the January 2005 X-class flares, *Astrophys. J.*, *673*, 1169.
- Stevens, M., J. C. Kasper, B. Maruca and A. J. Lazarus (2009), Development and application of advanced spectral analysis tools for Wind SWE, *Eos, Trans. AGU*, *90*(52), SH33B-1503.
- Tan, L. C., D. V. Reames, C. K. Ng, O. Saloniemi and L. Wang (2009), Observational evidence on the presence of an outer reflecting boundary in the solar energetic particle events, *Astrophys. J.*, *701*, 1753.
- Tu, C.-Y., E. Marsch and Z.-R. Qin (2004), Dependence of the proton beam drift velocity on the proton core plasma beta in the solar wind, *J. Geophys. Res.*, *109*, A05, 101.
- Verdini, A. and M. Velli (2007), Alfvén waves and turbulence in the solar atmosphere and solar wind, *Astrophys. J.*, *662*, 669.
- Viall, N. M., L. Kepko and H. E. Spence (2008), Inherent length-scales of periodic solar wind number density structures, *J. Geophys. Res.*, *113*, A07101, doi:10.1029/2007JA012881.
- Viall, N. M., H. E. Spence and J. C. Kasper (2009), Are periodic solar wind number density structures formed in the solar corona?, *Geophys. Res. Lett.*, *36*, L23102, doi:10.1029/2009GL041191.
- Wang, L., R. P. Lin, S. Krucker and J. T. Gosling (2006), Evidence for double injections in scatter-free solar impulsive electron events, *Geophys. Res. Lett.*, *33*, L03106.
- Wang, L., R. P. Lin, S. Krucker and G. M. Mason (2010a), A Statistical Study of Solar Electron Events over One Solar Cycle, *Astrophys. J.*, submitted.
- Wang, L., R. P. Lin, S. Krucker and G. M. Mason (2010b), Solar Injection of Ten Impulsive Electron/3He-rich SEP Events, *Astrophys. J.*, submitted.
- Wang, L., R. P. Lin and S. Krucker (2010c), Pitch angle distributions and temporal variations of 0.3-300 keV solar impulsive electron events, *Astrophys. J.*, submitted.
- Wilson III, L. B., C. A. Catell, P. J. Kellogg, K. Goetz, K. Kersten, L. Hanson, R. MacGregor and J. C. Kasper (2007), Waves in interplanetary shocks: a Wind/WAVES study, *Phys. Rev. Lett.*, *99*, 041, 101, doi:10.1103/PhysRevLett.99.041101.
- Wilson III, L. B., C. A. Catell, P. J. Kellogg, K. Goetz, K. Kersten, J. C. Kasper, A. Szabo and K. Meziane (2009), Low-frequency whistler waves and shocklets observed at quasi-perpendicular interplanetary shocks, *J. Geophys. Res.*, *114*, 10,106, doi:10.1029/2009JA014376.
- Wilson III, L. B., C. A. Catell, P. J. Kellogg, K. Goetz, K. Kersten, J. C. Kasper and A. Szabo (2010), Large amplitude electrostatic waves observed at a supercritical interplanetary shock, *J. Geophys. Res.*, doi:10.1029/2010JA015332.

APPENDIX A: STEREO/IMPACT - WIND E/PO PROGRAM

Solar Wind Outreach: STEREO/IMPACT-WIND

Previous and On-going FY10 work

Over the past two years, STEREO/IMPACT and *Wind* Education and Public Outreach efforts have pooled resources toward common goals to: 1) engage the public in solar wind science using *Wind* and STEREO/IMPACT data and sounds made from this data; 2) increase the public's awareness of the solar wind, coronal mass ejections, and the effect of the solar wind and CMEs on Earth's systems; and 3) to increase the use of our magnetism activities in classrooms around the country. In an attempt at meeting our first two goals, we have given talks on the solar wind in the context of sounds and science (UCLA sounds and science public conference webcast talks (archived at: <http://artsci.ucla.edu/sound/> under 'video archive'), through the San Francisco Exploratorium's podcasts ([http://www.exploratorium.edu/webcasts/archive.php?cmd=browse &project=87](http://www.exploratorium.edu/webcasts/archive.php?cmd=browse&project=87)), and the Astronomical Society of the Pacific Amateur Astronomy Network for the International Year of Astronomy. There are more talks planned for this coming FY10 year. We are also currently working to debug the most recent sonification software that was field-tested at a public event at the Exploratorium in order to more widely disseminate this program that turns solar wind data into sounds that attempt to represent the type of data being heard. Starting from the IMPACT E/PO website, we created a new solar wind website highlighting IMPACT, *Wind*, and ACE missions and science (working with the ACE E/PO lead: http://cse.ssl.berkeley.edu/stereo_solarwind/) To meet our second goal, we have presented the solar wind magnetism activities at the California Science Teachers Association conferences, taught the lesson to 150 middle school students in Piedmont, CA, and partnered with the Lawrence Hall of Science FOSS team to educate Oakland, CA elementary teachers about electricity and magnetism and physical science, using both hands-on activities and the 'story' of solar storms and their affect on Earth. A description of the IMPACT pre-launch programs is found in the more general STEREO E/PO paper [Peticolas *et al.*, 2007]. We are in the process of evaluating our most current sonification software product as a formative evaluation in order to update the product.

Future Plans: The main plans for the solar wind component of the *Wind*-STEREO E/PO program are to 1) keep current the solar wind website, sonification products, and magnetism lessons and 2) disseminate these products and the science discoveries as widely as possible given the financial constraints by a) working with the overall *Wind*-STEREO E/PO team to make the best use of resources and events, b) leveraging other NASA-funded E/PO programs, and c) presenting at teacher workshops already being organized by other organizations (such as the California Science Teachers Association conference and Sacramento Municipal Utility District.)

In all years (FY11-14), Dr. Peticolas will attend local science team meetings and ensure that the *Wind* and IMPACT teams share press releases and science discoveries to be then shared in appropriate language on the website and as talks to teachers during professional development workshops or through amateur astronomy networks, such as the Night Sky Network of the ASP. A student and Igor Ruderman (programmer) will work with Dr. Peticolas to maintain the solar wind website, keeping it up-to-date and also connecting it with other sun-related websites such as those on Wikipedia and NASA websites, such as the ACE E/PO website, Cosmicopia.

In FY11, Dr. Peticolas will update the solar wind lesson to better meet the needs of middle school teachers and their students based on previous teacher feedback on this lesson.

In FY11-12, Dr. Peticolas will work with ROSES EPOESS programs, Navajo Sky and Surfin' the solar wind, to help modify existing IMPACT-*Wind* resources for these NASA-funded programs that have components related to the Sun.

References

Peticolas, L.M., N. Craig, T. Kucera, D. J. Michels, J. Gerulskis, R. J. MacDowall, K. Beisser, C. Chrissotimos, J. G. Luhmann, A. B. Galvin, L. Ratta, E. Drobnes, B. J. Méndez, S. Hill, K. Marren, and R. Howard (2007), The STEREO Education and Public Outreach Program, *Space Sci. Rev.*, ISN 0038-6308 (Print) 1572-9672 (Online), doi: 10.1007/s11214-007-9287-y.

Summary Budget

Mission	FY11	FY12	FY13	FY14	Mission Total
<i>Wind</i>	\$20,084	\$19,946	\$20,013	\$20,024	\$80,067
STEREO/IMPACT	\$10,011	\$9,958	\$9,971	\$9,922	\$39,862
Total	\$30,095	\$29,904	\$29,984	\$29,946	\$119,929

Wind E/PO Budget

	FY11	FY12	FY13	FY14
1. Direct Labor (salaries, wages and fringe benefits)	\$12,342	\$12,591	\$12,841	\$13,099
2. Other Direct Costs:				
a. Subcontract				
b. Consultants	\$2,000	\$2,000	\$2,000	\$1,900
c. Equipment				
d. Supplies				
e. Travel	\$702	\$350	\$150	\$0
f. Other				
3. Facilities and Administrative Costs	\$5,040	\$5,005	\$5,022	\$5,025
4. Other Applicable Costs				
5. SUBTOTAL -- Estimated Costs	\$20,084	\$19,946	\$20,013	\$20,024
6. Less Proposed Cost Sharing				
7. Total E/PO Estimated Costs	\$20,084	\$19,946	\$20,013	\$20,024

Wind E/PO Budget Justification

Direct Labor: In all FY years, Dr. Laura Peticolas is budgeted 8% of her time per month (2% from IMPACT =10% per month in total – see IMPACT budget.) Dr. Laura Peticolas will provide direction to the project, coordinate activities, provide contact with the *Wind* science team, provide scientific content to resource updates, interact with other programs leveraged, and update lessons.

FY11: (0.96 month/year @ \$6,267/month = \$6,267) + (21% benefits and 4% retirement benefits, 25% benefits = \$1,567); FY11-14, 2% cost of living increase on salary each year: FY12: \$6,393 + \$1,598; FY13: \$6,520+\$1,630; FY14: \$6,651+\$1,663.

Dan Zevin will manage the overall program, help gather and track evaluation data, and interact with the evaluator. FY11: (0.60 month/year @ \$5,525/month = \$3,315) + (32% benefits and 4% retirement benefits, 36% benefits = \$1,193); FY11-14, 2% cost of living increase on salary each year: FY12: \$3,382 + \$1,218; FY13: \$3,449+\$1,242; FY14: \$3,518+\$1,266.

Other Direct Costs

Consultants: \$2,000 in FY11-13 and \$1,900 in FY14 to an evaluator to help analyze data and provide support writing evaluation reports.

Travel: FY11: \$702 (\$150 air; 3 nights and 3 days, \$120 lodging; \$64 per diem) to CSTA in Southern CA; FY12: \$350 for CSTA in Bay Area for ground transportation and local transportation to support other teacher workshops and outreach events; FY13: \$150 for ground transportation to support local teacher workshops and outreach events.

F&A costs: The Berkeley F&A costs for education and outreach programs is currently 33.5%. Graduate student fees are excluded from the base. The rate is effective 7/1/07-6/30/11 and provisional from 7/1/11 until amended. Cognizant Federal agency and official: DHHS Office of Inspector General, Office of Audit Services, Audit Manager, 90-7th Street, Suite 3650, San Francisco, CA 94103; tel. (415) 437-8360.

STEREO IMPACT E/PO Budget

	FY11	FY12	FY13	FY14
1. Direct Labor (salaries, wages and fringe benefits)	\$6,201	\$6,260	\$6,320	\$6,382
2. Other Direct Costs:				
a. Subcontract				
b. Consultants				
c. Equipment				
d. Supplies	\$2,310	\$2,298	\$2,301	\$2,290
e. Travel				
f. Other				
3. Facilities and Administrative Costs	\$2,310	\$2,298	\$2,301	\$2,290
4. Other Applicable Costs				
5. SUBTOTAL -- Estimated Costs	\$10,011	\$9,958	\$9,971	\$9,922
6. Less Proposed Cost Sharing				
7. Total E/PO Estimated Costs	\$10,011	\$9,958	\$9,971	\$9,922

STEREO IMPACT E/PO Budget Justification

Direct Labor: Dr. Peticolas is budgeted 2% of her time per month (8% from *Wind* =10% per month in total – see *Wind* budget.) Dr. Laura Peticolas will provide direction to the project, coordinate activities, provide contact with the *Wind* science team, provide scientific content to resource updates, interact with other programs leveraged, and update lessons. FY11: (0.24 month/year @ \$6,267/month = \$1,567) + (21% benefits and 4% retirement benefits, 25% benefits = \$392); FY11-14, 2% cost of living increase on salary each year: FY12: \$1,598 + \$400; FY13: \$1,630+\$408; FY14: \$1,663+\$416;

Igor Ruderman, Program Analyst, is budgeted for 1% of his time per month to support technical aspects of updating the website. FY11: (0.12 month/year @ \$6,022/month = \$723) + (34% benefits and 4% retirement benefits, 38% benefits = \$275); FY11-14, 2% cost of living increase on salary each year: FY12: \$737 + \$280; FY13: \$752+\$286; FY14: \$767+\$292.

An undergraduate student is budgeted for 1.2 months per year of his or her time to help maintain the solar wind website and make edits to the solar wind teacher lesson document, including 508 compliance (@ \$15/hour = \$3,120 per year each year for FY11-14.)

Other Direct Costs:

Supplies: Teacher workshop supplies (to support *Wind* budget to do teacher workshops), including photocopying and printing of CD-ROMs with magnetism and solar wind lessons on them for each year: FY11 \$1500, FY12 \$1400, FY13 \$1350, FY14 \$1250.

F&A costs: The rate 30% is effective 7/1/02 and will remain fixed at that level for the life of the contract award (which includes non-competing budget periods). Cognizant Federal agency and official: DHHS Office of Inspector General, Office of Audit Services, Audit Manager, 90-7th Street, Suite 3650, San Francisco, CA 94103; tel. (415) 437-8360.

APPENDIX B: WIND LEGACY MISSION ARCHIVE PLAN

Early in its mission, *Wind* and the other GGS spacecraft relied on a very capable and extensive science operations center, the Science Planning and Operations Facility (SPOF). The SPOF was responsible for the collecting, distribution and active archiving of all level zero (LZ) and ancillary data products. The SPOF also ran daily the instrument team provided data processing software to produce quick turn around, publicly available data, termed Key Parameters (KPs). The SPOF also provided science planning and software maintenance services.

With the passage of time, and with reducing funding levels, The SPOF had to be turned off and most of its functions were passed on to the instrument teams and to a small GSFC operation, the *Polar-Wind-Geotail* or PWG system, that continued to perform some LZ and KP functions. This unavoidable decentralization resulted in a degree of unevenness and disparity between the various *Wind* instrument data services. To solve this problem, key *Wind* instrument team members rallied around the new distributed Heliophysics Data Environment (HDE) concept and became funding members of the Virtual Heliospheric Observatory (VHO). The VHO provides a single point of entry for data without the costly necessity of a dedicated science operations center. The VHO also encourages its members to adopt the common SPASE dictionary based metadata standard thus providing the user community uniform descriptions of instruments and data products.

The development of the HDE and VHO is still ongoing, and not every *Wind* data product is yet at the level where the team would like it to be. Nevertheless, here we describe our current status and our plans to present the *Wind* data products independently usable thus achieving their full science potential.

Mission Operations Center. The *Wind* Mission Operations Center (MOC) resides at Goddard. It is currently still the remnant of the joint *Polar*, *Wind* and *Geotail* center under the Space Science Mission Operations (SSMO) contract. After the April, 2008 retirement of the *Polar* spacecraft, maintaining this system became too costly and plans have been developed to implement a Multi-Mission Operations Center (MMOC), also at Goddard, that joins *Wind* with ACE and TRACE. The transition to the MMOC is imminent with a scheduled Operation Readiness Review (ORR) scheduled for March 31, 2010. The functionality of the new MMOC will be the same as that of the legacy MOC.

The primary responsibility of the MOC and MMOC is spacecraft commanding, trend and anomaly analysis, DSN scheduling, the maintenance of *Wind* Near-Real-Time (NRT) passes and LZ generation for each instrument and spacecraft housekeeping. In addition, the Goddard flight dynamics facility provides orbit and attitude solutions. The MOC/MMOC, in turn, sends all of these data products daily to the PWG system. After the transition to the MMOC, we do not anticipate making any further changes to the *Wind* mission operations.

The PWG System. The *Polar-Wind-Geotail* (PWG) system handles the active archiving of LZ and ancillary files and their distribution to the instrument teams and various active archives. The PWG system also performs the rapid KP data production for all instruments. It resides in the Sciences Directorate of Goddard under the direct control of the project scientist. The PWG system has been streamlined onto only two computers (a data server and a data processor) (with hot spares) and is fully automated to eliminate the need for data technicians. The system is maintained by one IT engineer at a fraction of FTE. This system also serves as the interface to the *Wind* NRT data stream, which is real time processed data during the daily ~2 hour long spacecraft telemetry contact times. This NRT data is available in numerical and graphical format at: <http://pwg.gsfc.nasa.gov/windnrt/>.

The PWG system distributes the instrument and spacecraft housekeeping LZ files to the instrument teams via FTP. All of these LZ and orbit/attitude files are also publicly accessible at <ftp://pwgdata.gsfc.nasa.gov/pub/>. Only the most recent 60 days are served in uncompressed format, but the whole mission is archived in GZip compression. Even though the deep archival of these data files are handled by NSSDC, the PWG system also backs up all LZ data at two physical locations and onto tapes, CDs and DVDs. It should

be noted that the whole *Wind* mission to date requires only 300GB of storage for the LZ data, so the backup requirements are not overwhelming.

At the beginning of the mission, all *Wind* instrument teams had to supply software to automatically process some portion of their data into science data products, the KP data. Even though the KP data is clearly not the best quality data the instrument teams produce, it enjoys great popularity because it is always available publicly within 24 hours of observation. The PWG system maintains this software library, with occasional support (as needed) from the instrument teams and automatically places all the KP data on <http://cdaweb.gsfc.nasa.gov>. A more detailed description of the various KP products is given at the instrument sections below.

The PWG system also keeps the Satellite Situation Center (SSCWeb) up to date with orbit information (<http://sscweb.gsfc.nasa.gov>). Thus all orbit graphics generated on SSCWeb are always up to date.

At this point, the only further development of the PWG system we are still planning is the backup capability to parse the instrument LZ files directly from the instrument telemetry, a function currently carried out by the MOC. Should further cuts be necessary at the MMOC, we will investigate whether this function could be transferred to the PWG system at a reduced cost.

Instrument Data. The bulk of the instrument data processing and data dissemination takes place at the instrument sites. Next, each instrument team's effort is described. To aid the user community, we have developed a *Wind* project web page (<http://wind.nasa.gov>) that identifies the entry point for each instrument data environment and provides some degree of common documentation. However, our long term goal is to fully integrate all of the *Wind* data products into the VHO, thus making the data not only easy to find but also uniformly described.

Instrument, Calibration and Data Production Documentation. During the past two years, a significant effort went into collecting documentations for all the *Wind* instruments. These have been made publicly accessible through the *Wind* project web page (<http://wind.nasa.gov>). The documentation includes original instrument papers, ground and in-space calibration results and the details of how the various data products are generated. An ever increasing number of *Wind* data products also have SPASE compliant VxO metadata descriptions. Our plan is to complete the VHO description of all *Wind* data products during the next two years.

SWE Ions. The PWG system, on receipt of the LZ data, immediately processes a KP data product for the SWE Faraday Cup (FC). This automated procedure uses a convected isotropic Maxwellian to fit to the reduced distribution functions collected by the FC. These 92-second time resolution ASCII data files are available to the public within 24 hours of the observations at the MIT instrument web site (http://web.mit.edu/space/www/wind/wind_data.html) and at CDAWeb. A despiked version of this data is also available at NSSDC's FTP Helper (<http://ftpbrowser.gsfc.nasa.gov>). 1-hour averages of this data is also available at the MIT instrument page. While the KP products were originally designed as browse, quick look data only, the quality proved to be so high that this data product became the primary science level data product of the FC sub-system.

Recently, a new data production algorithm was developed that employs a bi-Maxwellian fit and obtains anisotropic temperatures for protons and a separate fit for Alpha particles. The resulting data product (designated H1 by CDAWeb), also contains the simpler moment computations primarily to allow direct comparison with the ACE SWEPAM proton data. This 92-second time resolution data can be located in ASCII format at the MIT web page and at FTPHelper, and in CDF format at CDAWeb.

A new FC data product, the reduced distribution functions in physical units with all instrument effects folded in, is being considered for development. Obviously, this data exists (this is what is fitted for the KP and H1 data) but is internal to the data production software. Due to its complexity on a rotating platform, this information was originally not planned to be publicly distributed. However, recently – encouraged by the development of new metadata standards that can handle complex data sets – the generation of the

reduced distribution functions was reinvestigated. This would be the most fundamental and complete presentation of the FC measurements. It is however, a major undertaking, and at the current low funding level of the instruments, it proceeds at a very slow pace. It is our plan that within two years the first test data products would be available. All of the FC data products are archived at the SPDF active archive.

SWE Ion Data Product	Time Res.	Time Coverage	Format	Location
KP protons (K0)	92 sec	1994/11/17-Present	ASCII	MIT, FTPHelper
			CDF	CDAWeb
KP protons	1 hour	1994/11/17-Present	ASCII	MIT
Bi-Maxwellian (H1)	92 sec	1995/1/1-(~6 mo lag)	ASCII	MIT, VHO
			CDF	CDAWeb

MIT: http://web.mit.edu/space/www/wind/wind_data.html

FTPHelper: <http://ftpbrowser.gsfc.nasa.gov>

SWE Electrons. All of the SWE electron data sets have been reprocessed during the last year. Due to a high voltage supply failure, the last available data from the VEIS detector is May 31, 2001. Since the Strahl detector has very similar capabilities, it was reprogrammed and the ground software rewritten to recover the electron moment and pitch angle measurements originally supplied by VEIS.

There are four types of SWE electron data products: (1) electron moments containing electron density, velocity, temperature and heat flux parameters; (2) the pitch angle files providing electron fluxes at 30 directional bins relative to the instantaneous magnetic field direction at 13 different energy levels; (3) the averaged pitch angle data product with various aggregate averages formed from the complete pitch angle data; (4) and finally the strahl data with higher angular resolution electron pitch angle observations near the magnetic field direction. Starting on Aug 16, 2002, all of these four data products are generated by a new production software based on the reprogrammed Strahl detector measurements. In addition, the electron 'moments' are no longer the result of integral moment calculations but estimated from the fitting of a single kappa distribution function to both the core and halo components.

SWE \bar{e} Data Product	Time Res.	Time Coverage	Format	Location
Moments (H0)	6-12 sec	1994/12/29-2001/5/31	CDF	CDAWeb, SWE, VHO
Pitch angle (H4)	6-12 sec	1994/12/29-2001/5/31	CDF	CDAWeb, SWE, VHO
Averaged pitch angle (M2)	6-12 sec	1994/12/29-2001/5/31	CDF	CDAWeb, SWE, VHO
New 'moments' (H2, H5)	12-15 sec	2002/8/16-Present	CDF	CDAWeb, SWE, VHO
New pitch angle ((H3)	12-15 sec	2002/8/16-Present	CDF	CDAWeb, SWE, VHO
New ave. pitch angle (M0)	12-15 sec	2002/8/16-Present	CDF	CDAWeb, SWE, VHO
New strahl (M1)	12-15 sec	2002/8/16-Present	CDF	CDAWeb, SWE, VHO

SWE: <ftp://windswe.gsfc.nasa.gov/pub>

3DP. As most *Wind* instruments, 3DP team has provided a KP production software to be run automatically at the PWG system. This data product contains electron and ion fluxes at seven energies for each particle and some basic moment computations and can be found at CDAWeb for the whole duration of the mission. Much more popular is the unique 3 second time resolution proton moment (PM) data. Even though it is computed on-board the spacecraft, as a result of ever improving calibration tables uploaded, it has proven very reliable. It can be accessed for the complete mission at the 3DP instrument site, at CDAWeb and through VHO. In addition, the 24-second time resolution ion omni-directional fluxes and the 98-second electron omni-directional fluxes can also be obtained at both the 3DP and CDAWeb sites. Electron and proton pitch angle distributions and SST energy spectra are currently available only at the 3DP site. However, work is already ongoing to transfer these data sets also to CDAweb.

3DP Data Product	Time Res.	Time Coverage	Format	Location
KP	92 sec	Whole mission	CDF	CDAWeb
PM on-board proton moments	3 sec	Whole mission	CDF	CDAWeb, Berkeley, VHO
ELSP \bar{e} omnidirectional flux	98 sec	Whole mission	CDF	CDAWeb, Berkeley
PLSP proton omnidirectional flux	24 sec	Whole mission	CDF	CDAWeb, Berkeley
ELPD \bar{e} pitch angles	98 sec	Whole mission	CDF	Berkeley, VHO
PLPD proton pitch angles	24 sec	Whole mission	CDF	Berkeley
SFSP SST \bar{e} energy spectra	12 sec	Whole mission	CDF	Berkeley
SOSP SST proton energy spectra	12 sec	Whole mission	CDF	Berkeley

Berkeley: <http://sprg.ssl.berkeley.edu/wind3dp>

SMS. Till the failure of the SWICS instrument (May 27, 2000), combined SWICS and STICS KP files were generated that contain alpha particle information along with some carbon and oxygen abundances and temperatures. This data product is still publicly available from CDAWeb. Since the SWICS failure, a lot of time went into determining how to properly use the other two sensors by themselves. A new software system has been developed which automates many data analysis functions previously done manually. Development of this system is in the data validation and optimization stage, with the first scientific analyses already underway. Daily averages of the proton and alpha particle phase space density distribution functions for the whole mission is already publicly available through the *Wind* project web page. In addition, hourly resolution STICS and MASS energy spectra for select days throughout the mission are available in digital and graphical formats from the University of Michigan page (http://solar-heliospheric.engin.umich.edu/mission_db/spectra.php?craft=2). Further work is under way to produce more data products.

SMS Data Product	Time Res.	Time Coverage	Format	Location
KP SWICS+STICS	4 hours	1994/12/12-2000/5/27	CDF	CDAWeb
STICS p+ α distr. function	1 day	1995/1/1-2007/12/31	ASCII	Wind project
STICS+MASS spectra	1 hour	Select days	ASCII	U. Michigan

U. Michigan: http://solar-heliospheric.engin.umich.edu/mission_db/spectra.php?craft=2

EPACT. Fluxes for a select number of ions (helium, oxygen, iron and combined CNO) in energy bins below 1 Mev/nuc and averaged over 92 seconds are publicly available for the whole mission in KP files at CDAWeb. Recently, a systematic search for events with non-zero count rates have been undertaken, and 41 such several day long periods identified in the 1997-2003 time range. For these intervals hourly resolution omnidirectional intensity data (OMN) and ion sectored count data (SEC) were generated. These ASCII text files are publicly available at the *Wind* project web page. In addition, a process has begun to compute the first order ion anisotropy from these observations. The results for the first five events are also available from the *Wind* project web page. This effort will continue and more event files will be made public once the Sun becomes more active again. Also we are working on a new format that will make more species available throughout the whole mission.

EPACT Data Product	Time Res.	Time Coverage	Format	Location
KP fluxes	92 sec	1994/11/16-Present	CDF	CDAWeb
OMN omnidirectional flux	1 hour	41 events	ASCII	Wind project
SEC sectored counts	1 hour	41 events	ASCII	Wind project
Anisotropy	1 hour	5 events	ASCII	Wind project

MFI. The MFI team essentially generates only one kind of data product, the vector magnetic fields, at various time resolutions and with increasing quality of calibrations. Within 24 hour of measurement, the

92-second KP data is publicly available at CDAWeb. This data uses periodically updated calibration tables. Typically, with no longer than 1 week delay the MFI team produces a calibrated data product that includes 3-second, 1 minute and 1 hour averages. This data product (version 3) has the final calibrations in the spacecraft spin plane. Requiring at least of 6 months of time lag, a final calibrated data, with spin axis corrections typically of no more than a few tenth of a nT, are also generated (version 4). This final data has the same format as the version 3 files. To encourage the use of the higher quality data products, CDAWeb keeps only the latest year of KP data on-line. The version 4 files also replace version 3 files at both the CDAWeb and on the instrument web page (<http://lepmfi.gsfc.nasa.gov>). The VHO is also serving the version 3 and 4 files.

Till recently, the full 11 or 22 vectors/sec data was too large in volume to serve on-line and has been stored on tapes and made publicly available on request. Currently, there is an ongoing effort to further reduce artificial spin tones in this high time resolution data and package it for web distribution. A new algorithm is already in the testing stage.

MFI Data Product	Time Res.	Time Coverage	Format	Location
KP	92 sec	Most recent 1 year	CDF	CDAWeb
Calibrated version 3	3 sec, 1min, 1 hour	1994/11/16-1 week lag	CDF	CDAWeb, MFI, VHO
Definitive version 4	3 sec, 1min, 1 hour	1994/11/16-6 months lag	CDF	CDAWeb, MFI, VHO
High time resolution	11 or 22 vec/sec	1994/11/16-Present	ASCII	On request

MFI: <http://lepmfi.gsfc.nasa.gov>

WAVES. As most other *Wind* instruments, WAVES also produces a KP data product that is immediately publicly available at CDAWeb. The WAVES KP data contains 3-minute averages of the electric field intensities at 76 log-spaced frequencies and electron density estimates based on neural network determined electron plasma frequency values. In addition, the team produces, with no more than 1 week delay, higher time resolution (1 minute) normalized receiver voltages and makes it available both at CDAWeb and on their own web site. This is the fundamental data product that is used for the generation of the familiar WAVES frequency vs. time intensity plots. These plots are also pre-generated and publicly available on the instrument web page in PDF format. Finally, 7-10 second time resolution electron density estimates are also computed and made available at CDAWeb. WAVES data products will be described by VWO. The WAVES team also maintains a Type II/IV catalog on their web site that is widely used.

Software Tools. Unlike the other *Wind* instrument teams, the WAVES team distributes primarily the lowest level data they have without generating many higher level products. Therefore, dedicated software tools are necessary for non-specialists to make use of this data. The team maintains a small IDL software library on their web site that readily ingests the downloaded IDL save files and allows the custom generation of data plots.

WAVES Data Product	Time Res.	Time Coverage	Format	Location
KP	3 min	1994/11/10-Present	CDF	CDAWeb
Rad1, Rad2, TNR	1 min	1994/11/10-Present	ASCII, IDL save	CDAWeb, WAVES
High res electron density	7-10 sec	1994/11/10-Present	CDF	CDAWeb
Rad1, Rad2 plots	1 min	1994/11/10-Present	PDF	WAVES

WAVES: <http://www-lep.gsfc.nasa.gov/waves/>

KONUS and TGRS. The KONUS and TGRS γ -ray instruments are not maintained by heliophysics. Their data production and data distribution is completely handled by the astrophysics division. Description of the instruments and links to their data products can be found at (<http://heasarc.gsfc.nasa.gov/docs/heasarc/missions/wind.html>).

ACRONYMS

3D	three-dimensional
3DP	3D Plasma (experiment)
ACE	Advanced Composition Explorer
APE	Alpha-Proton-Electron (telescope)
AU	Astronomical Unit
CME	Coronal Mass Ejection
DSN	Deep Space Network
EPACT	Energetic Particles: Acceleration, Composition, and Transport
E/PO	Education and Public Outreach
FTE	Full Time Equivalent
GF	Giant Flares
GGS	Global Geospace Science
GOES	Geostationary Operational Environmental Satellites
GRBs	Gamma Ray Bursts
GSFC	Goddard Space Flight Center
HETE-2	High Energy Transient Explorer-2
HGO	Heliophysics Great Observatory
HI	Heliospheric Imagers
ICME	Interplanetary Coronal Mass Ejection
IMF	Interplanetary Magnetic Field
IMPACT	In-situ Measurements of Particles and CME Transients (suite)
IP	Interplanetary
IPN	Interplanetary GRB Network
ISTP	International Solar-Terrestrial Physics
IT (detector)	Isotope Telescope
ITOS	Integrated Test and Operations System
keV	kilo-electron volt
KONUS	Gamma-Ray Spectrometer
LASCO	Large Angle and Spectrometric COronagraph
LEMT	Low Energy Matrix Telescopes
LET	Low Energy Telescope
LWS	Living With a Star
MC	Magnetic Cloud
MESSENGER	Mercury Surface Space Environment Geochemistry and Ranging
MeV	Mega-electron volt
MHD	Magnetohydrodynamic
MMOC	Multi-Mission Operations Center
MMS	Magnetospheric Multi-Scale NASA STP mission
MOVE	Mission Operations Voice Enhancement
NASA	National Aeronautics and Space Administration
NSSDC	National Space Science Data Center
PWG	Polar Wind Geotail ground system
RBSP	Radiation Belt Storm Probes
RHESSI	Reuven Ramaty High Energy Solar Spectroscopic Imager
SDO	Solar Dynamics Observatory
SECCHI	Sun Earth Connection Coronal and Heliospheric Investigation

SEPs	Solar Energetic Particles
SGR	Soft Gamma Repeaters
SIS	Solar Isotope Spectrometer
SMD	Science Mission Directorate
SMS	SWICS-MASS-STICS (package on Wind)
SOHO	SOLar and Heliospheric Observatory
SPASE	Space Physics Archive Search and Extract
SSMO	Space Science Mission Operations
STEP	SupraThermal Energetic Particle Telescope
STEREO	Solar-Terrestrial Relations Observatory
STICS	SupraThermal Ion Composition Spectrometer
SWE	Solar Wind Experiment
SWICS	Solar Wind Ion Composition Spectrometer
TGRS	Transient Gamma-Ray Spectrometer
THEMIS	Time History of Events and Macroscale Interactions During Substorms
TPOCC	Transportable Payload Operations Control Center
TRACE	Transition Region And Coronal Explorer
ULEIS	Ultra Low Energy Isotope Spectrometer
VDS	Voice/Video Distribution System
VEIS	Vector Ion-Electron Spectrometers
VHO	Virtual Heliophysics Observatory
VWO	Virtual Waves Observatory
WYE	Work Year Equivalent